

MACROSCOPIC PROPERTIES OF EQUITY MARKETS: STYLIZED FACTS AND PORTFOLIO PERFORMANCE

STEVEN CAMPBELL, QIEN SONG, AND TING-KAM LEONARD WONG

ABSTRACT. Macroscopic properties of equity markets affect the performance of active equity strategies but many are not adequately captured by conventional models of financial mathematics and econometrics. Using the CRSP Database of the US equity market, we study empirically several macroscopic properties defined in terms of market capitalizations and returns, and highlight a list of stylized facts and open questions motivated in part by stochastic portfolio theory. Additionally, we present a systematic backtest of the diversity-weighted portfolio under various configurations and study its performance in relation to macroscopic quantities. All of our results can be replicated using codes made available on our GitHub repository.

1. INTRODUCTION

The development of quantitative finance and financial practice goes hand in hand with the analysis of financial data. Over the last few decades, academic researchers and practitioners have accumulated an enormous amount of empirical work on the temporal behaviours of individual and multiple asset prices at low and high frequencies, as well as cross-sectional properties in relation to macroeconomic, fundamental and statistical factors. Cont's 2001 paper [27] summarizes many by now classical *stylized facts* about individual assets. Also see [7, 17, 61, 88, 113] for textbook accounts of financial econometrics and empirical asset pricing theory. More recent developments include but are not limited to modelling of market microstructures and limit order books [64], rough volatility [63], signature-based models [32], econophysics [24], machine learning techniques in asset pricing [65], energy markets [30, 99] as well as cryptocurrencies and decentralized finance [28, 122]. These results not only improve our understanding of financial markets but also directly affect the design, implementation and risk management of trading strategies, especially for new markets and products. In each context, knowledge of stylized facts is essential since they highlight key properties that a realistic model should capture. Despite the variety of markets, equity markets remain fundamental because of their sheer sizes and primary functions of financing and trading of risks.

In this paper we study empirically a collection of *macroscopic properties* of equity markets which are highly relevant in the management of large equity portfolios but are not adequately addressed by the aforementioned literature. In a nutshell, a macroscopic quantity or property of an equity market is one which depends on all or a majority of the stocks in the market. The most basic example is the total market capitalization, or overall performance, of the market which is well represented by a capitalization-weighted market index such as the S&P 500. The index often serves as a benchmark for equity portfolios, both passive and active, and may be approximated by tradeable assets such as exchange-traded funds. Our terminology is motivated by statistical physics in which one considers macroscopic quantities such as volume, temperature and pressure. To take our crude physical analogy a bit further, suppose we think of an equity market as a galaxy and each stock as a star. Then the market index is a proxy of the total mass, but there are other interesting macroscopic quantities, such as the shape, spiral and rotation of the galaxy, which affect and are affected by

Key words and phrases. capital distribution, market diversity, excess growth rate, intrinsic volatility, backtesting, diversity-weighted portfolio, stochastic portfolio theory, stylized facts.

the stars, and are much less understood.¹ From the viewpoint of, say, the manager of an equity portfolio which aims to outperform a capitalization-weighted benchmark, macroscopic properties are clearly relevant since they affect both the absolute performance of the strategy and the relative performance with respect to the benchmark. For example, in [2, 47] it was shown empirically that changes in *market diversity* (Section 3.2), which measures the concentration of the market capitalization weights, correlate significantly with the relative return of actively managed large-cap portfolios. Macroscopic properties are also related to the overall stability of the market [23]. Viewing equity markets from the macroscopic perspective suggests many interesting questions which are not satisfactorily captured by conventional models of asset prices. The study of macroscopic features and their relationship with individual actions also arises in other areas in mathematical finance and applied probability, most notably in *mean-field games* [21, 66, 67, 85].

Our study is motivated by *stochastic portfolio theory* (SPT) which was first pioneered by Fernholz [47, 51, 58]. This mathematical theory provides a fresh perspective on some macroscopic properties of large equity markets, especially those defined in terms of market capitalizations and/or returns. In particular, market diversity and *intrinsic volatility* (relative volatility among the stocks, see Section 4), appear to be stable over long periods and, at least under suitable conditions, can be exploited by carefully chosen portfolios to outperform a capitalization-weighted benchmark. While the size factor has played an important role in empirical finance (see e.g. [43]), SPT places great emphasis on how (relative) sizes simplify the modelling of the market, describe its stability, and allow us to analyze in depth the relative performance of a wide class of systematically rebalanced portfolios. Unfortunately, many results motivated by SPT remain largely inaccessible to non-experts due to their technical nature and possibly some restrictions imposed by the mathematical models (such as the interacting particle systems discussed in Section 3.1 and the focus on functionally generated portfolios). Also, the majority of papers in SPT focus on theoretical developments. Many important empirical questions, such as the joint modelling and prediction of diversity and volatility, and the calibration and diagnostics of high dimensional market models, are largely open.

Our paper, whose title is inspired by [27], has three main objectives. First and foremost, we present a self-contained and unified empirical study of some macroscopic properties of the US equity market from 1962 to 2023, based on the CRSP US Stock Database, for a broad audience including financial mathematicians, econometricians, financial economists and portfolio managers. We substantiate, and sometimes modify, the “folklore observations” in SPT, thereby suggesting a collection of statistical and financial problems that we believe are of interest to the aforementioned communities. We summarize our main empirical findings which will be made more precise in the body of the paper:

- 1. Capital distribution curve is stable:** The dependence of market capitalization weight on relative rank (by size) does not follow Zipf’s law but has been stable over decades.
- 2. Market diversity is maintained through entrances and exits of stocks.** The capital distribution of a fixed collection of stocks tends to become more concentrated over time.
- 3. Cross-sectional volatility clusters in time and correlates with change in market diversity:** The relative volatility among stocks exhibits ARCH effects and tends to be high when market concentration changes quickly.
- 4. Smaller stocks are more volatile and tend to become (relatively) smaller.** Smaller stocks have systematically larger absolute volatilities, cross ranks more often, and has a higher tendency to be overtaken by smaller or new stocks.

To facilitate replication of our empirical results and/or modification of the conventions and parameters adopted, we have made our codes publicly available.² Second, we perform a systematic

¹There are also other galaxies (markets) but they are beyond the scope of this paper.

²See <https://github.com/stevenacampbell/Macroscopic-Properties-of-Equity-Markets>. The CRSP Data, which is licensed, must be obtained separately.

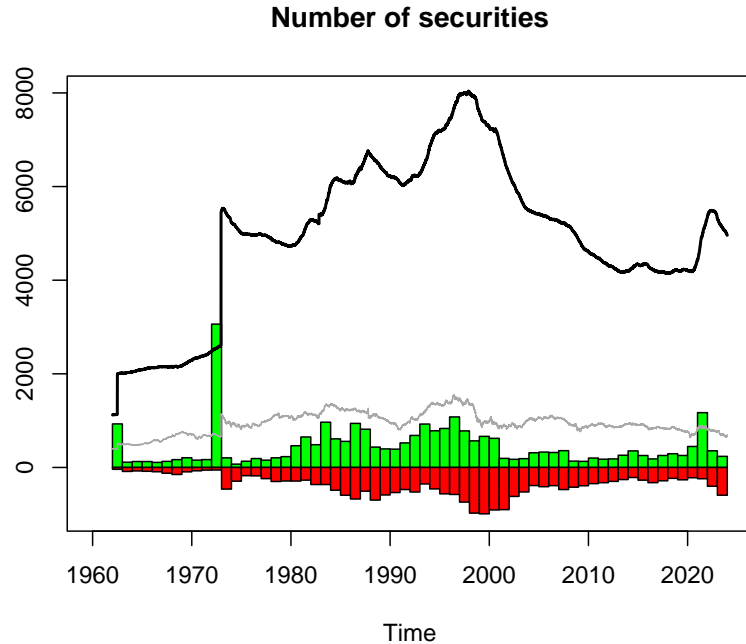


FIGURE 1. Overview of our CRSP data-set. Black (thick) series: Number of stocks in the full universe. Grey (thin) series: Minimum number of stocks to cover at least 90% of total market capitalization. Green (positive) bars: Number of new stocks. Red (negative) bars: Number of stocks delisted from the universe. The first two series are daily and the last two are yearly. The jumps in 1962 and 1972 are technical adjustments due to the inclusion of NYSE American and NASDAQ stocks.

empirical backtesting of various specifications of the *diversity-weighted portfolio* [53] which is a representative large cap, rule-based strategy of special interest in portfolio management in general, and in SPT in particular. We show how their performance, relative to a capitalization-weighted benchmark, depend on the (realized) macroscopic quantities, extending the empirical studies in [105, 111]. Our backtesting engine, which implements the algorithm in [105] for long-only portfolios under proportional transaction costs, is also available on our repository and may be useful to other researchers and practitioners. Third, as a by-product of our exposition, we offer discussions on recent developments motivated by SPT, extending beyond those covered in the 2009 survey [56], again with the broader communities in mind.

The rest of the paper is organized as follows. We begin by describing, in Section 2, the CRSP dataset of the US stock market and introduce some notations which will be used throughout the paper. Section 3 is concerned with the capital distribution curve and market diversity. In Section 4 we study the market’s excess growth rate which is a measure of intrinsic volatility and examine how it relates with market diversity. Section 5 considers how the behaviours of stocks depend systematically on their relative ranks. Our portfolio backtesting experiments are presented in Section 6. Finally, in Section 7 we summarize our findings and discuss several directions for future research. Although knowledge of SPT is not assumed for reading this paper, we include for completeness a brief but self-contained overview of its main ideas in Appendix A. In Appendix B we recall the definition of local time which motivates the quantities studied in Section 5.3.

2. DATA

In this paper we focus on the US equity market for which detailed daily data is provided by the Center for Research in Securities Prices (CRSP).³ The CRSP database contains, among other attributes, the daily market capitalizations and returns of traded stocks listed on major US exchanges including NYSE, NYSE American, NASDAQ, NYSE Arca and BATS. Dividends, corporate actions and delisting events are also included. We recommend Ruf's Python notebooks [104] for an accessible tutorial of the database. Following [105], we restrict to *common stocks* (more precisely, the securities with CRSP share codes (`shrcd`) 10, 11 and 12) and exclude other securities such as closed-end funds and REITs. While the data of NYSE stocks dates back to December 1925, stocks from NYSE American were included in CRSP starting July 1962 (and NASDAQ stocks in December 1972). NYSE Arca stocks were added in March 2006 but the effect was minor. For the purposes of this paper our data-set consists of the common stocks in the CRSP database from 1962-01-02 to 2023-12-29. Figure 1 provides an overview of our CRSP data-set. For each trading day t , let \mathcal{A}_t be the set of all stocks which are traded on day t ; we call it the *CRSP universe* on day t and emphasize that it varies over time. We may think of each $i \in \mathcal{A}_t$ as the name or unique identifier of a listed company. As will be seen later, the inflow and outflow of stocks are highly relevant to the stylized features as well as the overall stability of the market. For $i \in \mathcal{A}_t$, let $X_i(t) > 0$ be the market capitalization of stock i at the start of day t ; it is, by definition, the product of the stock price and the number of outstanding shares. Despite the large number of stocks, the majority of market capital is concentrated in a relatively small number of the largest stocks. For example, throughout 2000–2023 the largest 1000 stocks generally represent more than 90% of the total market capitalization $\sum_{i \in \mathcal{A}_t} X_i(t)$. The concentration of capital among the stocks can be quantified using the concept of *market diversity* (Section 3.2).

3. CAPITAL DISTRIBUTION CURVE AND MARKET DIVERSITY

3.1. The capital distribution curve. Let $\mathcal{I}_t \subset \mathcal{A}_t$ be a given collection of stocks on day t . For $i \in \mathcal{I}_t$, the *capitalization weight* of stock i relative to \mathcal{I}_t is defined by

$$(3.1) \quad \mu_i^{\mathcal{I}_t} = \mu_i^{\mathcal{I}_t}(t) := \frac{X_i(t)}{\sum_{j \in \mathcal{I}_t} X_j(t)}, \quad i \in \mathcal{I}_t.$$

The capitalization weights define a probability vector with values in the (closed) *unit simplex*

$$\mathcal{P}(\mathcal{I}_t) = \left\{ (\mu_i)_{i \in \mathcal{I}_t} : \mu_i \geq 0, \quad \sum_{i \in \mathcal{I}_t} \mu_i = 1 \right\},$$

and can be regarded as the portfolio weights of a capitalization-weighted index. Nevertheless, naive implementation of this capitalization-weighted portfolio can be costly because of turnovers.⁴ Neglecting corporate events (such as dividends and delisting), a stock's capitalization weight increases (resp. decreases) if it outperforms (resp. underperforms) relative to the capitalization-weighted index.

Using the capitalization weights, we can visualize more accurately and vividly the evolution of the CRSP universe. In Figure 2, we show with each green dot (left panel) the time and size of a stock when it is newly listed, and with each red dot (right panel) the same information for a stock which is delisted forever or for an extended period. We observe that both “births” (entrances) and “deaths” (exits) occur frequently across a wide range of market capitalizations, yet their intensities appear to fluctuate over time. The weights at exit time are overall more spread out than the weights

³The CRSP US Stock Databases can be accessed on the following website: <https://www.crsp.org/products/research-products/crsp-us-stock-databases>.

⁴*Index tracking*, which is the main objective of passive portfolio management, is a topic of substantial practical importance, see e.g. [20, 110] and the references therein.

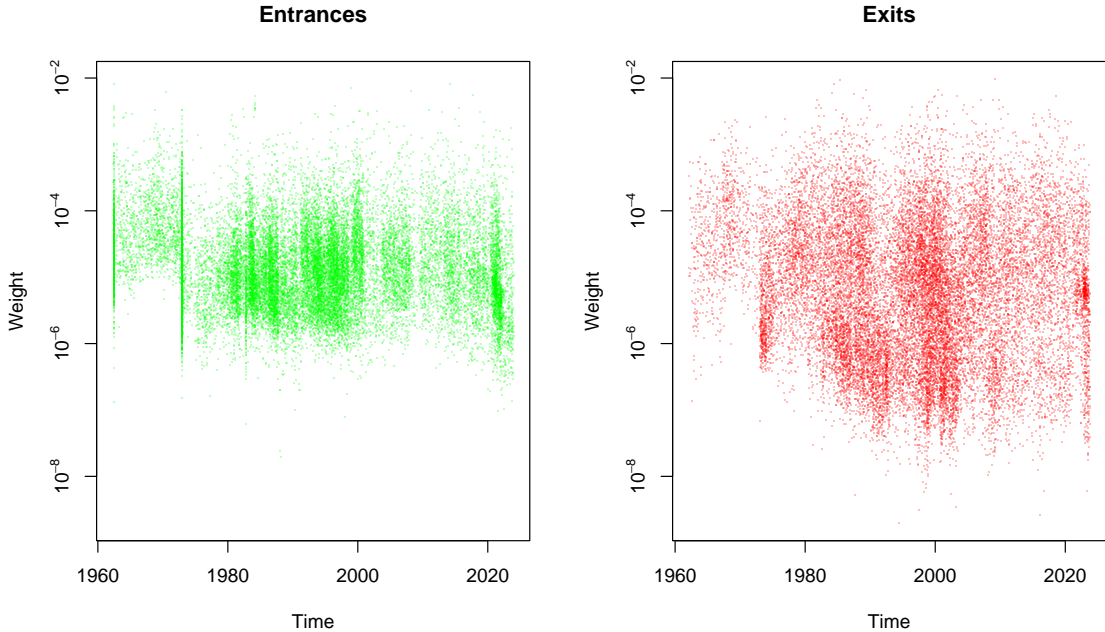


FIGURE 2. Inflow (left) and outflow (right) of the CRSP universe. Each green dot shows the time and capitalization weight (relative to the full CRSP universe) when a new stock enters the market. The red dots do the same for stocks which leave the market. The vertical green “strips” in 1962 and 1972 correspond to two artificial enlargements of the CRSP universe.

at entrance. An interesting statistical problem is to relate these fluctuations with the underlying economy such as business cycles.

The *capital distribution* relative to \mathcal{I}_t is defined as the *ranked* probability vector

$$(3.2) \quad \mu_{\geq}^{\mathcal{I}_t} = (\mu_{(1)}^{\mathcal{I}_t}, \mu_{(2)}^{\mathcal{I}_t}, \dots, \mu_{(|\mathcal{I}_t|)}^{\mathcal{I}_t}),$$

where $\mu_{(1)}^{\mathcal{I}_t} \geq \mu_{(2)}^{\mathcal{I}_t} \geq \dots \geq \mu_{(|\mathcal{I}_t|)}^{\mathcal{I}_t}$ are the capitalization weights ($\mu_i^{\mathcal{I}_t}$) arranged in descending order. Since $\mu_{(k)}^{\mathcal{I}_t}$ decays rather quickly as k increases, the capital distribution is usually visualized in log-log scale, i.e., $\log \mu_{(k)}^{\mathcal{I}_t}$ against $\log k$. We call the graph of $\log k \mapsto \log \mu_{(k)}^{\mathcal{I}_t}$ the *capital distribution curve* relative to the given universe (we use base 10 for plotting purposes). When $\mathcal{I}_t = \mathcal{A}_t$ is the full universe, we call it the *full* capital distribution curve.

In Figure 3 we plot the full capital distribution curve, which is one of the most iconic objects in SPT (see e.g. [47, Chapter 5]), from 1962 to 2023. The evolving dimension of \mathcal{A}_t is inconvenient for conventional statistical methods. To avoid this issue, one may restrict to the subuniverse \mathcal{A}_t^K consisting of the largest K stocks of \mathcal{A}_t ;⁵ this amounts to renormalizing $(\mu_{(1)}^{\mathcal{A}_t}(t), \dots, \mu_{(K)}^{\mathcal{A}_t}(t))$. The capital distribution curves relative to \mathcal{A}_t^K with $K = 1000$ are visualized collectively in Figure 4 as a *surface* over the (log rank)-date plane. A glance at Figures 3 and 4 should convince the reader that the capital distribution curve is a rather delicate object to model faithfully - either directly or through a *market model* which specifies the joint dynamics of all stocks. Here, we observe that the left end of the curve is more volatile (in log-scale) than the right end, even though smaller stocks are generally more volatile in absolute terms (see [18, Section 5.3] and Section 5). Nevertheless,

⁵Exact ties occur extremely rarely, if at all, and can be resolved arbitrarily.

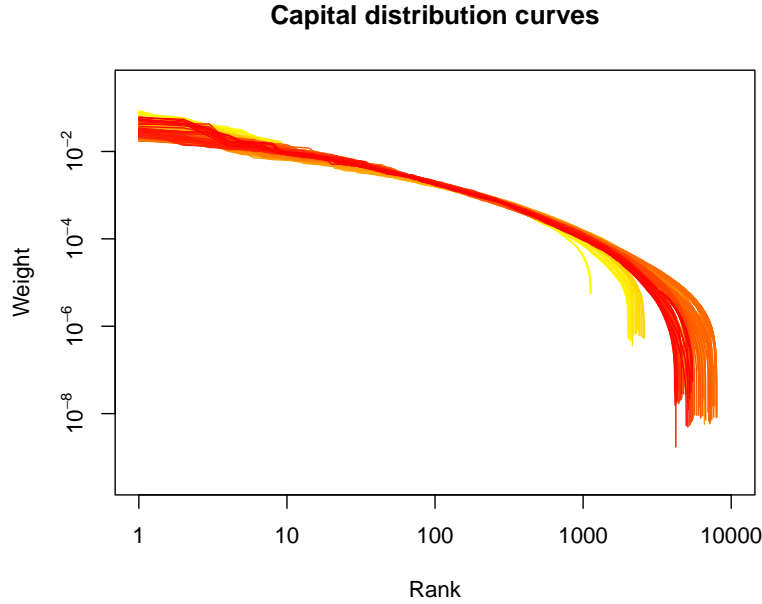


FIGURE 3. Capital distribution curves from 1962–2023 of the full CRSP universe. The curves are colored from yellow (more distant) to red (more recent).

the overall shapes of the capital distribution curves appear to be quite stable. Thus we state our first stylized fact, somewhat loosely, as follows:

Stylized Fact 1. *The overall shape of the capital distribution curve is stable. In particular, the full capital distribution curve is generally concave and decays rapidly on the right end.*

The apparent long-term stability, which we distinguish from the concept of (strict or second order) *stationarity* in time series analysis, of the shape of the capital distribution curve is striking and calls for explanation. As noted in [37, pages 101–103], this stability is neglected by standard multivariate financial models. To take a simple example, suppose stocks followed a multivariate Black-Scholes model as in the classical Merton problem [92]. Then the capital distribution would eventually degenerate into a point mass by the law of large numbers. If the capital distribution followed approximately a *power law* (or *Pareto distribution*) with exponent $\alpha > 0$, i.e., $\mu_{(k)}^{A_t} \approx \frac{1}{Z_t} k^{-\alpha}$ where Z_t is a normalization constant, the capital distribution curve would look approximately like a straight line with slope $-\alpha$. The special case $\alpha = 1$ is frequently called *Zipf's law*. While power laws are ubiquitous in many rank–size distributions in economics (see e.g. [59, 62, 94, 106] and the references therein) and complex systems [112], it does not hold for the full capital distribution curve but may be a reasonable first approximation. Here, we should mention that the CRSP universe does not contain private companies which are not listed on stock exchanges. We also remark that because the capital distribution curve is plotted in log-log scale, a visually small change of the curve, especially on its right end, correspond to large movements in the capitalization weights.

A possible interpretation of the stability of shape is that the capital distribution curve, which may be regarded as a high dimensional time series, can be well approximated by a low dimensional object which is stable in some sense. This suggests the use of dimension reduction. Using *convex principal component analysis* [13] which can incorporate the monotone constraint of the capital distribution (3.2), the first and the last author showed in [18, Section 6.3] that by restricting to, say, the largest 1000 stocks (which differ from day to day) and using the *Aitchison geometry* [40] on the (ranked) unit simplex, about 80% of the variation of the curve can be captured by

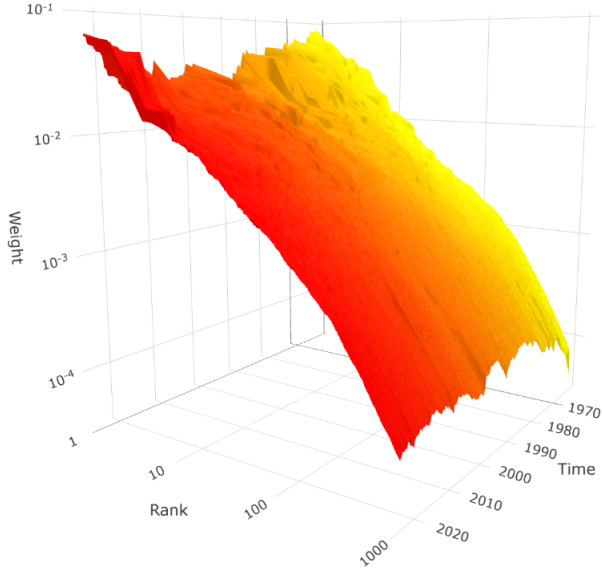


FIGURE 4. Capital distribution curves of the top 1000 stocks from 1962–2023, visualized collectively as a surface. Colored from yellow (more distant) to red (more recent).

the first two convex principal components. Moreover, movements along the first convex principal component correlate strongly with *market diversity* whose behaviours are examined in Section 3.2. Nevertheless, dimension reduction methods generally cannot capture idiosyncratic behaviours of the stocks, especially the largest ones which have significant influence on the market.

Consider the problem of constructing stochastic models of market capitalizations which are capable of reproducing some features of the observed capital distribution curve (and ideally other behaviours of the market). A reasonably realistic model not only improves our understanding of the market but also serves as a *scenario generator* for optimizing and backtesting trading and risk management strategies. To enforce stability, a far-reaching idea, first proposed by Fernholz in [47, Section 5.5] based on empirical observations, is to let the dynamics of a stock depend on its rank. This modelling assumption motivated novel *rank-based diffusions*, and related processes such as *volatility-stabilized processes* and *polynomial processes*, for which a substantial probabilistic literature has accumulated in the last two decades (see e.g. [8, 26, 31, 33, 55, 59, 68, 69, 74, 84, 95, 108, 109] and their references). While it is beyond the scope of this paper to describe the variety of mathematical results obtained, we will explain the main ideas.

For theoretical tractability, one typically considers an equity market consisting of a fixed (finite or countably infinite) collection of stocks; in particular, IPOs and delisting events are neglected even though they are prominent as seen in Figure 1.⁶ Nevertheless, by considering the largest $K \leq n$ stocks of the system, one can obtain a simulated universe which evolves over time via rank switchings.⁷ As a basic example, we mention the *generalized Atlas model*, introduced in [8], under which the market capitalizations $X_1(t), \dots, X_n(t)$ of n stocks are modelled in continuous time as a Markov diffusion process satisfying the following system of stochastic differential equations:

$$(3.3) \quad d \log X_i(t) = \sum_{k=1}^n \gamma_k \mathbb{1}_{\{\text{rank}_i(t)=k\}} dt + \sum_{k=1}^n \sigma_k \mathbb{1}_{\{\text{rank}_i(t)=k\}} dW_i(t), \quad i = 1, \dots, n,$$

⁶A notable exception is [80] which studied models with splits and mergers.

⁷The subsystem consisting of the largest K stock is called an *open market* in [78].

where $\text{rank}_i(t)$ is the rank of stock i at time t , γ_k and σ_k are suitable *rank-based* constants and W_1, \dots, W_n are independent Brownian motions. In words, (3.3) says that the log market capitalization, $\log X_i$, of stock i has drift γ_k and volatility σ_k when it has rank k at time t . Focusing on rank-based behaviours limits the number of parameters. For example, the system (3.3) is specified by $2n$ parameters while an unrestricted covariance matrix requires $\frac{1}{2}n(n+1)$. In Section 5 we report some empirical evidence of rank dependence. *Interacting particle systems* such as (3.3) are not straightforward to analyze since the coefficients are discontinuous in the state variable.⁸ Also, the dynamics of the *ranked* market weights $\mu_{(k)}(t)$ and the *gaps* $\log \mu_{(k)}(t) - \log \mu_{(k+1)}(t)$ involve delicate concepts such as local times, collisions, as well as, reflections over polyhedral boundaries. Under suitable structural conditions on the parameters, it can be shown that a process such as (3.3) is ergodic and has a unique stationary distribution, under which the (expectation of the) capital-distribution curve is qualitatively similar to the ones shown in Figure 3. They also capture some other rank-based properties such as the *higher volatility of smaller stocks* (Section 5.1). Nevertheless, we observe that most, if not all, results in this literature rely on ergodicity in the limit $t \rightarrow \infty$ and the stationary distribution. Consequently, these models need not, and usually do not, capture (qualitatively or quantitatively) short and medium term behaviours of the observed equity market.

The model in (3.3) is called a *first order* model since the coefficients depend only on the ranks. A *second order* or *hybrid* model, as in [54, 69, 74] involves also *name-based* coefficients and can incorporate idiosyncratic features. Calibration of ranked-based and volatility-stabilized market models to market data, as done in [47, 55, 68, 69, 73], is typically based on ad hoc methods analogous to moment matching and elementary estimates of growth rates and volatility coefficients (with smoothing); accuracy of the estimates and diagnostic checks are not addressed. A natural problem is to improve these models, their calibration and predictive power, possibly using tools in machine learning such as *neural stochastic differential equations* (see e.g. [87]). Moreover, market models such as (3.3) are *exogenous*; they do not explain why and how the stated dynamics emerge from interactions of the investors and the underlying economy. An ambitious goal is to come up with economically sound models of the financial market under which the observed macroscopic features emerge. Ideas from *evolutionary finance* [14, 42], *mean-field games* [22, 70, 76, 85] and *complex systems* [112] may be relevant in modelling the dynamics of firms and interactions among investors and/or their strategies.

3.2. Market diversity. *Diversity indexes* are used in various fields to quantify the complexity or concentration of a system or population consisting of multiple “species”. Examples include the Gini index for wealth inequality in economics, Hill numbers for biodiversity in ecology, and entropy as a measure of randomness in information theory and statistical physics. A comprehensive mathematical treatment can be found in [86].⁹ For an equity market, a natural idea is to quantify the diversity of the capitalization weights $\mu^{\mathcal{I}_t}(t) = (\mu_i^{\mathcal{I}_t}(t), i \in \mathcal{I}_t)$ as a probability vector indexed by the names, or the capital distribution $\mu_{\geq}^{\mathcal{I}_t}(t)$ as a probability vector indexed by the ranks, by an entropy-like measure. In this context, the first paper we are aware of is [49], in which the Shannon entropy was used. Unless otherwise stated, in this paper we measure market diversity of a collection \mathcal{I}_t of stocks by the *Shannon entropy* of $\mu^{\mathcal{I}_t}(t)$ defined by

$$(3.4) \quad \mathbf{H}(\mu^{\mathcal{I}_t}(t)) := - \sum_{i \in \mathcal{I}_t} \mu_i^{\mathcal{I}_t}(t) \log \mu_i^{\mathcal{I}_t}(t).$$

By symmetry of the entropy we have $\mathbf{H}(\mu^{\mathcal{I}}(t)) = \mathbf{H}(\mu_{\geq}^{\mathcal{I}_t}(t))$. For a universe with a *fixed size* $|\mathcal{I}_t|$, $\mathbf{H}(\mu(t))$ is maximized (with value $\log |\mathcal{I}_t|$) when $\mu(t)$ is the uniform distribution, i.e., $\mu_i^{\mathcal{I}_t}(t) = \frac{1}{|\mathcal{I}_t|}$,

⁸In (3.3) the coefficients are piecewise constant. Existence of a weak solution follows from the theory in [10].

⁹We thank Martin Larsson for pointing us to this interesting reference.

and is minimized (with value 0) when some stock completely dominates the universe, i.e., $\mu_i^{\mathcal{I}_t}(t) = 1$ for some i and $\mu_j^{\mathcal{I}_t}(t) = 0$ for $j \neq i$. Apart from the Shannon entropy, other diversity measures (see [47, Section 3.4]) may be used and produce qualitatively similar results; a specific example is the parameterized diversity measure \mathbf{D}_p defined by

$$(3.5) \quad \mathbf{D}_p(\mu^{\mathcal{I}_t}(t)) := \left(\sum_{i \in \mathcal{I}_t} (\mu_i^{\mathcal{I}_t}(t))^p \right)^{\frac{1}{p}},$$

where $p \in (0, 1)$ is a tuning parameter. It is closely related to the *Rényi entropy* (see [119, Proposition 2]) and the *diversity-weighted portfolio* (A.7) whose performance will be backtested, under various specifications, in Section 6. In fact, under the classical setting in SPT, the change in $\log \mathbf{D}_p$ is a major component of the relative performance of the diversity-weighted portfolio with respect to the market portfolio, in the short to medium term (see (A.8)). More generally, in [2] (also see [52, 53]) it was shown that the diversity of the S&P 500 – which corresponds roughly to \mathcal{A}_t^{500} – correlates significantly with the average relative performance of large-cap managers. Additional empirical results will be reported in Section 6.

Being a summary statistic of the capital distribution, market diversity is related to the shape of the capital distribution curve. Roughly, diversity is higher when the curve is “flatter” and is lower when the curve is “steeper”. In [18] we used convex PCA to make this idea precise: market diversity correlates strongly with the projection of the capital distribution curve onto the first convex principal component (analogous to how the the first and second principal components of yield curves can usually be interpreted in terms of the “level” and the “slope” of the curve). Since the capital distribution curve is “stable” by Stylized Fact 1, it is natural to expect that market diversity has a tendency to decrease when it is “too high” and a tendency to increase when it is “too low”. This idea is often expressed in the following

Stylized Fact (Folklore). *Market diversity (quantified by, say, the Shannon entropy) is mean-reverting.*

In the following we show that the behaviours of market diversity depend crucially on the *choice of the universe* \mathcal{I}_t . On the other hand, that diversity is “mean reverting” is subject to doubt. In the strictest sense, mean reversion means diversity is well approximated by an autoregressive or Ornstein-Uhlenbeck process about a fixed (or possibly varying) equilibrium level. While our empirical results do not provide conclusive evidence of this claim, long-term probabilistic behaviours of diversity and other observables can be analyzed mathematically for rank-based systems which generalize (3.3); see [93].

In the top panel of Figure 5 we show the time series of the diversity $\mathbf{H}(\mu^{\mathcal{A}_t}(t))$ of the *full* CRSP universe. Observe that $\mathbf{H}(\mu^{\mathcal{A}_t}(t))$ correlates to some extent with $|\mathcal{A}_t|$, the total number of stocks (see Figure 1). This is due to a *size effect* in the entropy (and other reasonable measures of diversity) [86]. For example, for $K \geq 1$ and $\alpha > 0$, consider the ranked probability vector $\mu_{(\cdot)} = (\mu_{(k)})_{k=1}^K$ where $p_k = \frac{1}{Z_{K,\alpha}} k^{-\alpha}$ follows a power law with exponent α (here $Z_{K,\alpha} = \sum_{k=1}^K k^{-\alpha}$ is the normalizing constant). Then one can verify that for $\alpha > 0$ fixed, $\mathbf{H}(p)$ is monotonically increasing in K .¹⁰ Thus it is difficult to argue that $\mathbf{H}(\mu_t^{\mathcal{A}}(t))$ has a fixed long term equilibrium value to which diversity is reverting. Intuitively, we might expect that a diverse market is more resilient to sudden shocks and catastrophic events, but the relation between diversity and systemic risk is, to the best of our knowledge, largely open. Also see [75] for a comparative study of the systemic risks of international equity markets using a skewness-based measure.

¹⁰On the other hand, the size effect may outweigh an increase in overall concentration. For example, if $p_k = Z_{K,\alpha} k^{-\alpha}$, $1 \leq k \leq K$ and $p'_k = Z_{K',\alpha'} k^{-\alpha'}$, $1 \leq k \leq K'$, are two Pareto distributions where $K' > K$ and $\alpha' > \alpha$, it is possible to have $\mathbf{H}(p') > \mathbf{H}(p)$.

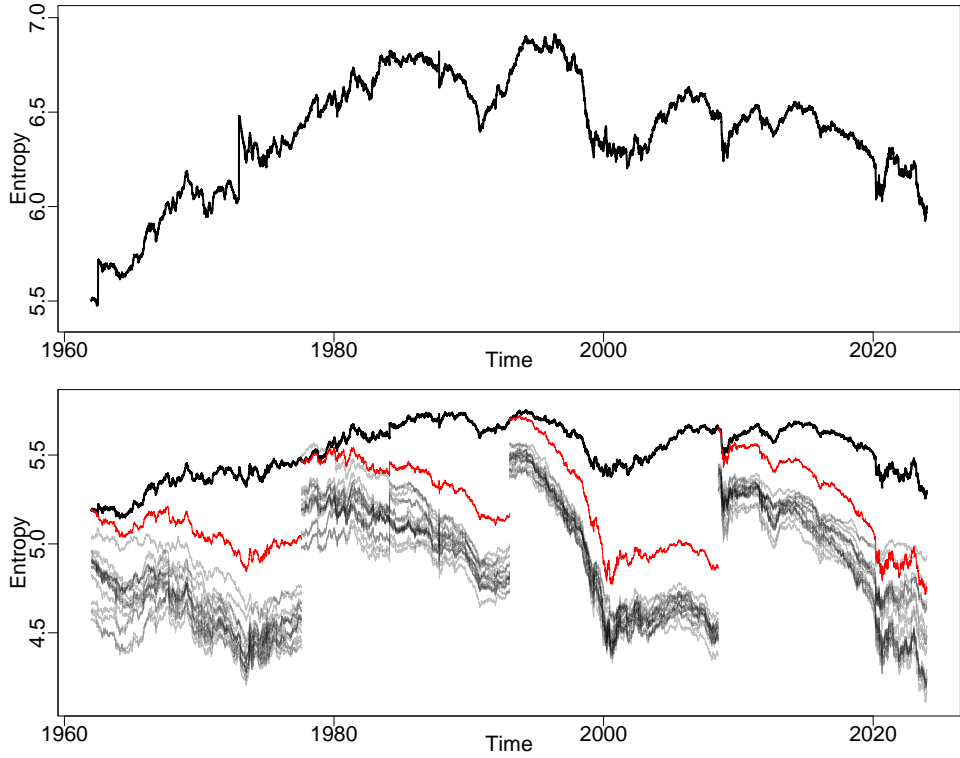


FIGURE 5. Diversities (entropies) of several universes. Top: Full CRSP universe. Bottom: (i) (black) largest 500 stocks, renewed daily; (ii) (red) largest 500 stocks, renewed at the start of each subinterval; (iii) (grey) 25 randomly chosen collections, each containing 500 stocks, renewed for each subinterval.

Observe that in 2023, even after the COVID-19 recession, the diversity of \mathcal{A}_t dropped to the lowest level since the 1970s. The recent decrease in market diversity, largely attributable to seven mega-capitalization stocks, dubbed the ‘‘Magnificent Seven’’, is affecting active managers’ stock selection behaviour. The *active-share ratio*, which measures how active portfolios deviate from the benchmark S&P 500, is at its lowest level since 2013 [115], indicating that active portfolio managers are choosing to mimic the benchmark more because missing out on any of the top-weighted stocks can lead to underperformance. If this trend continues, the (left end of the) capital distribution curve will look slightly steeper than before.

Next consider the behaviour of $\mathbf{H}(\mu^{\mathcal{I}_t}(t))$ for suitably chosen subuniverses \mathcal{I}_t with $|\mathcal{I}_t| \leq K$; this makes it more straightforward to interpret the change in diversity over time. In the bottom panel of Figure 5 we consider three cases where $K = 500$:

- (i) (Black series) $\mathcal{I}_t = \mathcal{A}_t^K$ is the largest K stocks on day t renewed every day. Now diversity fluctuates in a much tighter interval compared to the case of full universe, but even with this restriction it is difficult to argue the existence of a fixed equilibrium value. Note that during the period 1962–1972 the CRSP universe was artificially enlarged twice due to the addition of NYSE American and NASDAQ stocks. The diversity of \mathcal{A}_t^K increased rather steadily in this period. We also observe that diversity appears to exhibit short to medium term trends or momentum. Also, several sudden drops in market diversity are associated with market crashes such as the financial crisis in 2008 and COVID-19 in 2020.
- (ii) (Red series) We divide the whole period 1962–2023 into 4 subintervals $[t_i, t_{i+1}]$ (about 15.5 years each). For t in $[t_i, t_{i+1}]$, we let $\mathcal{I}_t = \mathcal{A}_{t_i}^K \cap \mathcal{A}_t$, i.e., the (still existing) stocks which

were one of the largest K on day t_i . (Note that $|\mathcal{I}_t| < K$ if some of the stocks were delisted before day t .) Interestingly, we see that *diversity generally decreases* in all subintervals. In other words, the capital distribution with respect to \mathcal{I}_t tends to become more and more concentrated. Intuitively, this is due to the widely differing growth rates of the stocks.

(iii) (Grey series) For each subinterval $[t_i, t_{i+1}]$ in (ii), we pick K stocks \mathcal{I}_{t_i} randomly in $\mathcal{A}_{t_i}^M$, where $M = 1000$, and, for $t \in [t_i, t_{i+1}]$, let $\mathcal{I}_t = \mathcal{I}_{t_i} \cap \mathcal{A}_t$. That is, we track the diversity of the randomly chosen stocks as a closed system. We generate 25 batches for each subinterval. Again we see that the diversity of \mathcal{I}_t generally decreases over time. Also, the randomly selected subuniverses are generally less diverse than $\mathcal{A}_{t_i}^K \cap \mathcal{A}_t$, which in turn is generally less diverse than \mathcal{A}_t^K .

Since the capital distribution is “stable” and diversity is a function of the capital distribution, we may say, rather vaguely, that “diversity is stable” as a corollary to Stylized Fact 1. Saying “diversity is mean reverting” requires the existence of a (possibly varying) equilibrium value which we fail to establish convincingly. On the other hand, we summarize the results of (ii) and (iii) in the stylized fact:

Stylized Fact 2. *Diversity of a fixed collection of stocks tends to decrease over time.*

To better understand the results in (ii) and (iii), consider Figure 6 in which we track the ranks of three groups of 50 stocks over the period 2010–2020. The initial ranks of the groups are respectively $1 \leq k \leq 50$, $201 \leq k \leq 250$ and $1001 \leq k \leq 1050$. We see that the top group, corresponding to the largest companies, remain mostly on top even after 10 years. On the other hand, the ranks of the lower groups are much more volatile. For a fixed universe, this dispersion causes diversity to decrease over time, i.e., its capital distribution becomes more and more concentrated. More empirical properties related to ranks will be discussed in Section 5 where we identify an overall decreasing trend in the ranking of individual stocks and quantify the intensity of rank switching.

As a corollary of Stylized Fact 2, which summarizes (ii) and (iii), the apparent stability of the capital distribution, and hence diversity, is fueled by the constant entrances and exits of stocks over time. We emphasize that this observation is absent in the classical SPT model (which assumes a fixed collection of stocks) as well as rank-based diffusion models such as (3.3).

Due to the effect of market diversity in the relative performance of actively managed portfolios, a natural question is to predict its future values. In [6], the authors developed a generalized tree-structured model using macroeconomic information and reported outperformance in predictive power relative to standard time series methods. Even simple models may be quite useful. For example, the authors of [111] implemented a regression model (motivated by the theoretical decomposition (A.8)) to devise a rule to decrease the drawdown of the equal-weighted portfolio by switching to a capitalization-weighted portfolio when diversity is expected to drop. We note, however, that modelling diversity as a standalone time series is different from building a model for a system of stocks whose diversity exhibits realistic behaviours. Again, we stress the importance of economic models which explain why the capital distribution curve (and hence diversity) behaves in the way it does; they allow us to understand if the observed stability is truly a long term invariant or may shift subject to changes in the market (e.g. the rise of massive tech companies and artificial intelligence). Another interesting problem, which may be of practical interest, is to use option prices (of stocks, indices and ETFs) to infer market participants’ perceptions of future values of market diversity and possibly other quantities such as intrinsic volatility. Finally, we mention the problem of developing alternative measures of diversity which take into account additional features such as sectors and statistical similarities between different stocks.¹¹

¹¹This problem was suggested by Martin Larsson.

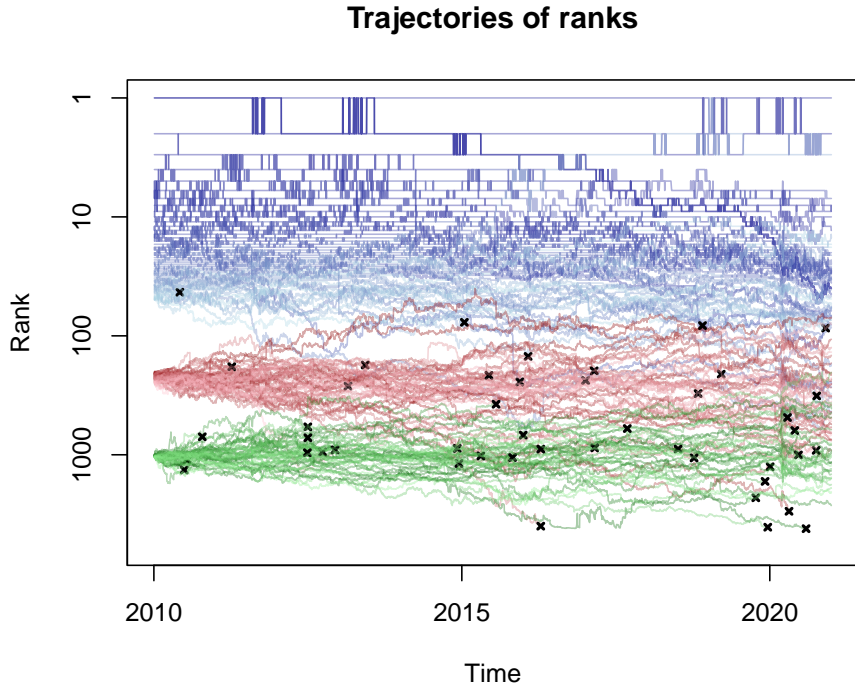


FIGURE 6. Ranks (in log-scale) of three groups of 50 stocks (blue, red, green) over the period 2010–2020. Delisting events are marked with crosses.

4. INTRINSIC MARKET VOLATILITY

The conventional or *absolute* aggregate volatility of an equity market usually refers to the volatility of its market index. For the US equity market, it is standard to use the past-looking historical volatility (e.g. standard deviation) of the returns of S&P 500 and the forward-looking VIX (CBOE Volatility Index) which is computed using option prices. In contrast, by *intrinsic* market volatility (following the terminology in [56]) we mean *relative volatility* among the stocks. For example, if all stocks go down by 20% there is large absolute volatility but no relative volatility – all equity portfolios yield the same return regardless of their weights. On the other hand, the market index may stay constant even if the stocks have widely differing returns. Thus relative volatility is *necessary* for an actively managed portfolio to outperform the market,¹² and provides complementary information about market behaviours relevant to trading decisions. In this section, we quantify intrinsic market volatility using the concept of *excess growth rate* [58], which is also known in the finance literature as the *diversification return* [15, 102].

4.1. Excess growth rate. We define the excess growth rate (EGR) using the formulation in [96, 97]. Consider a time interval $[t_0, t_1]$ and a collection $\mathcal{I}_{t_0} \subset \mathcal{A}_{t_0}$, such that stock $i \in \mathcal{I}_{t_0}$ has log-return $r_i(t_0, t_1) \in \mathbb{R}$ over $[t_0, t_1]$.¹³ Given a probability vector $w = (w_i)_{i \in \mathcal{I}_{t_0}} \in \mathcal{P}(\mathcal{I}_{t_0})$, we define the *excess growth rate* $\gamma_w(t_0, t_1)$ over $[t_0, t_1]$ and weighted by w , by

$$(4.1) \quad \gamma_w(t_0, t_1) := \log \left(\sum_{i \in \mathcal{I}_{t_0}} w_i e^{r_i(t_0, t_1)} \right) - \sum_{i \in \mathcal{I}_{t_0}} w_i r_i(t_0, t_1).$$

¹²See [48] for a theoretical study about its sufficiency.

¹³If $r_i(t_0, t_1) = -\infty$ and $w_i > 0$ then (4.1) gives $\gamma_w^*(t_0, t_1) = \infty$. The excess growth rate never blows up to ∞ in our computation.

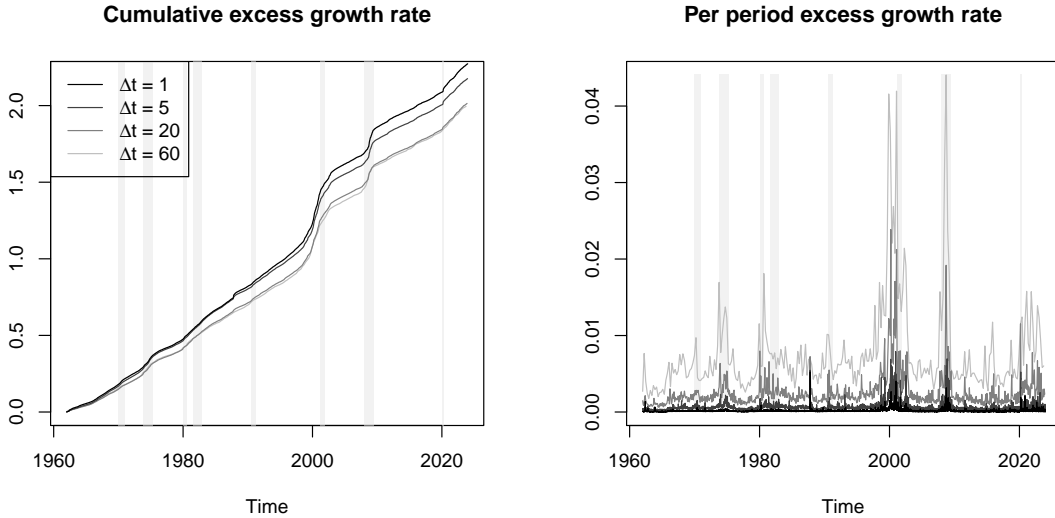


FIGURE 7. Left: Cumulative excess growth rate $\Gamma_w(t)$ for $w(t) = \mu_t^{\mathcal{A}_t^{1000}}$, at various frequencies. Right panel: Per period excess growth rate $\gamma_w(t_\ell, t_{\ell+1})$ for the same frequencies. The vertical shades indicate periods of recessions defined by the National Bureau of Economic Research.

Financially, $\gamma_w(t_0, t_1)$ is the difference between the log-return of the portfolio with weights (w_i) and the weighted average log return of the underlying assets; this explains why it is called the *excess* growth rate. Jensen's inequality implies that $\gamma_w(t_0, t_1) \geq 0$ and (when $w_i > 0$ for all i) $\gamma_w(t_0, t_1) = 0$ if and only if all $r_i(t_0, t_1)$ are the same. Thus we may regard $\gamma_w(t_0, t_1)$ as a measure of *realized* relative volatility over the period $[t_0, t_1]$. Common choices of w include the capitalization weights $w_i = \mu_i^{\mathcal{I}_{t_0}}(t_0)$ and the equal weights $w_i = \frac{1}{n}$, where $n = |\mathcal{I}_{t_0}|$. If we are given a time grid $\{t_\ell\}_{\ell \geq 0}$, universes $\{\mathcal{I}_{t_\ell}\}_{\ell \geq 0}$ and weights $w(t_\ell) \in \mathcal{P}(\mathcal{I}_{t_\ell})$, we define the *cumulative excess growth rate* $\Gamma_w(t)$ with respect to the given time grid and weights by $\Gamma_w(t_0) = 0$ and

$$(4.2) \quad \Gamma_w(t_\ell) = \Gamma_w(t_{\ell-1}) + \gamma_w(t_{\ell-1}, t_\ell), \quad \ell \geq 1.$$

In a continuous time framework where stock prices are modelled by continuous semimartingales (see Appendix A) the cumulative excess growth rate (as the partition size tends to zero) can be modelled in terms of a quadratic variation, see (A.2).

To further motivate the excess growth rate we discuss some of its properties:

- (i) The excess growth rate is *numéraire invariant*, i.e., γ_w remains unchanged if the asset prices, and hence their returns, are measured with respect to another numéraire such as a benchmark portfolio [96, Lemma 3.2]. This makes the excess growth rate an appropriate measure of relative volatility.¹⁴
- (ii) When $r_i(t_0, t_1) \approx 0$ for each i the following quadratic Taylor approximation holds:

$$(4.3) \quad \gamma_w(t_0, t_1) \approx \frac{1}{2} \left(\sum_{i \in \mathcal{I}_{t_0}} w_i r_i(t_0, t_1)^2 - \left(\sum_{i \in \mathcal{I}_{t_0}} w_i r_i(t_0, t_1) \right)^2 \right).$$

Thus $\gamma_w(t_0, t_1)$ can be approximated by half of the *variance* of the log returns of the stocks when weighted by w .

¹⁴Numéraire invariance uniquely characterizes the excess growth rate among a class of distance-like quantities called *L-divergences*; see [98, Example 3.10].

(iii) Fix a time grid $\{t_\ell\}$ with initial time T_0 and final time T_1 , $\mathcal{I} \subset \mathcal{A}_{T_0}$, and a probability vector w over \mathcal{I} . Summing (4.1) over time gives the decomposition

$$(4.4) \quad \log \left(\prod_{\ell} \sum_{i \in \mathcal{I}} w_i e^{r_i(t_\ell, t_{\ell+1})} \right) = \sum_{i \in \mathcal{I}} w_i r_i(T_0, T_1) + \Gamma_w(T_0, T_1),$$

which is the discrete analogue of (A.1). The left hand side of (4.4) is the log-return $r_w(T_0, T_1)$ of the portfolio rebalanced to the *constant* weight w at each time t_ℓ (here and in (iii) we neglect transaction costs). Everything else equal, a large relative volatility is favourable to a rebalanced portfolio compared to a capitalization-weighted one. This observation underlies the idea of *volatility pumping* [16, 38, 96, 102] and can be formalized mathematically using the concept of *functional portfolio generation* in SPT [47, 50, 97, 119].¹⁵ Thus it is natural to consider maximization of excess growth rate subject to suitable constraints [47, Example 1.1.7]. For example, risk-adjusted performance of portfolios optimized with respect to excess growth rate was investigated in [91], and a generalized efficient frontier was constructed in [39].

(iv) The excess growth rate depends on the *sampling* or *rebalancing frequency* which may be non-constant over time. For example, given three time points $t_0 < t_1 < t_2$ and w , the excess growth rate $\gamma_w(t_0, t_2)$ is generally different from the sum $\gamma_w(t_0, t_1) + \gamma_w(t_1, t_2)$. When the former is larger it is better not to rebalance.¹⁶ To explain this, suppose in the context of (ii) $\{\tilde{t}_m\}$ is another time grid over $[T_0, T_1]$. If $\tilde{r}_w(T_0, T_1)$ is the log return of the portfolio rebalanced to w at times \tilde{t}_m , then

$$(4.5) \quad r_w(T_0, T_1) - \tilde{r}_w(T_0, T_1) = \Gamma_w^*(T_0, T_1) - \tilde{\Gamma}_w^*(T_0, T_1),$$

where $\tilde{\Gamma}_w$ is the cumulated excess growth rate with respect to the time grid $\{\tilde{t}_m\}$. Thus the *spread* in (4.5) captures the effect of the frequency of rebalancing in the absence of transaction costs. The authors of [57] observed in a high-frequency setting that the cumulative excess growth rate increases as the frequency of rebalancing increases and devised a long-short hedging portfolio to exploit the spread.

4.2. Empirical results. In Figure 7 we consider the per period excess growth rate γ_w (right) and the cumulative excess growth rate Γ_w (left) at various frequencies, where $w(t) = \mu^{\mathcal{A}_t^K}(t)$ is the capitalization weights relative to the top $K = 1000$ stocks. We consider the frequencies $\Delta t = 1$ (daily), 5 (~weekly), 20 (~monthly) and 60 (~quarterly).¹⁷ We observe that the cumulative excess growth rate grows roughly linearly over time (about 3.5% per year when $\Delta t = 5$). Nevertheless, as seen in Figure 7 (right) and the sample autocorrelation function shown in Figure 8 (left), the excess growth rate exhibits clear ARCH effects at all frequencies considered, and is large during the financial crises in 2000 and 2008 among other significant market events. We stress that stochastic volatility of this sort is absent in all rank-based diffusion models studied so far, hence it is a promising direction to extend these models to capture the time series properties of relative volatility (alongside stability of the capital distribution curve).

Stylized Fact 3. *Market excess growth rate is correlated with absolute market volatility and exhibits an ARCH effect.*

¹⁵For a general portfolio (not constant weighted or functionally generated), pathwise decompositions such as (4.4) do not apply and a direct attribution of performance to its excess growth rate is less clear. See [25, 116] and the references therein for discussions about the limitations of the excess growth rate or diversification return in explaining “alpha”. In this section, we simply use the excess growth rate as a measure of intrinsic volatility. In Section 6 we relate the excess growth rate with the performance of the diversity-weighted portfolio which is functionally generated.

¹⁶A geometric interpretation based on a generalized Pythagorean theorem is given in [98].

¹⁷Here, and in the backtests in Section 6, we use constant intervals in trading days instead of calendar days to mitigate possible calendar effects.

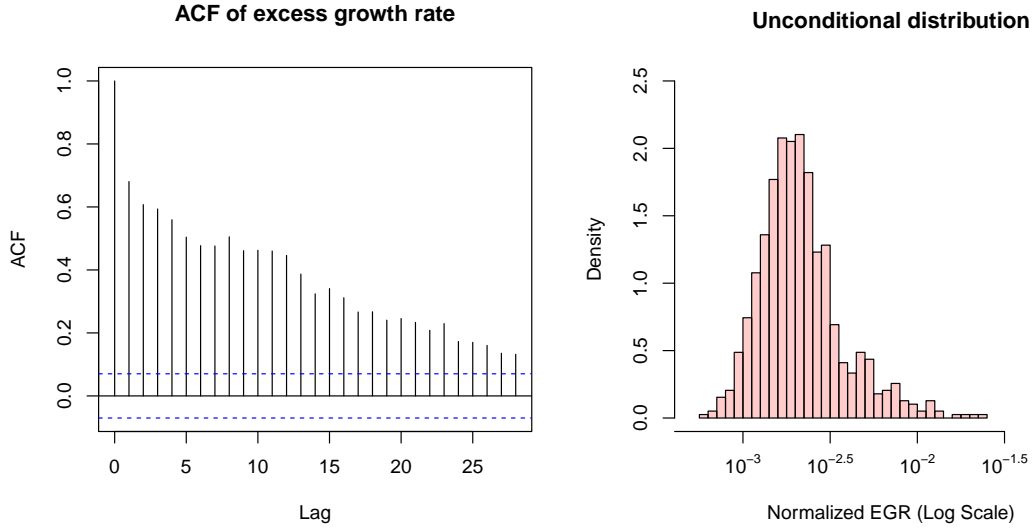


FIGURE 8. Empirical properties of $\gamma_w(t)$ in the context of Figure 7, where $\Delta t = 5$. Left: Sample autocorrelation function. Right: Unconditional distribution of (the logarithm of) $\frac{1}{\Delta t} \gamma_w(t, t + \Delta t)$.

The unconditional (marginal) distribution of the excess growth rate is highly skewed towards the right. In Figure 8(right) we plot the empirical distribution of the normalized excess growth rate $\frac{1}{\Delta t} \gamma_w(t, t + \Delta t)$ for $\Delta t = 5$ (the distributions for other frequencies are similar). The sample skewness of $\gamma_w(t, t + \Delta t)$ is 4.3 and the excess kurtosis is 27.3. There is moderate positive correlation between excess growth rate (relative volatility) and market (absolute) volatility. For example, for $\Delta t = 5$ the empirical correlation between γ_w and the squared capitalization-weighted return is about 0.41; the Winsorized version, which corrects for outliers, is about 0.25.¹⁸

Next we turn to joint behaviours of market diversity (here quantified by market entropy) and intrinsic volatility (excess growth rate). Recall that intrinsic volatility is necessary for a rebalanced portfolio (such as the diversity-weighted portfolio simulated in Section 6) to outperform a capitalization-weighted benchmark. However, such a portfolio is exposed to risks posed by changes in market diversity. In Figure 9 (left) we plot the daily excess growth rate γ_w (where w is the capitalization weight vector) and the daily change in diversity, again for the top 1000 stocks on each day. The underlying pattern is not visually obvious due to the large number of data points. A local regression (LOWESS) reveals a systematic dependence which is roughly symmetric in the sign of the change in diversity. The relationship is more evident if we zoom out in time. In Figure 9 (right) we consider instead time intervals with length $\Delta t = 20$ trading days. For each interval $[t_\ell, t_{\ell+1}]$, we plot the cumulative daily excess growth rate $\Delta \Gamma_w = \Gamma_w(t_{\ell+1}) - \Gamma_w(t_\ell)$ versus the range $\max_{t \in [t_\ell, t_{\ell+1}]} \mathbf{H}(\mu(t)) - \min_{t \in [t_\ell, t_{\ell+1}]} \mathbf{H}(\mu(t)) \geq 0$ of diversity. Again we observe a positive dependence. Thus we state the next stylized fact as follows:

Stylized Fact 4. *Excess growth rate tends to be larger when market diversity is volatile and vice versa.*

¹⁸We use here the function `corHuber()` from the R package `robustHD`.

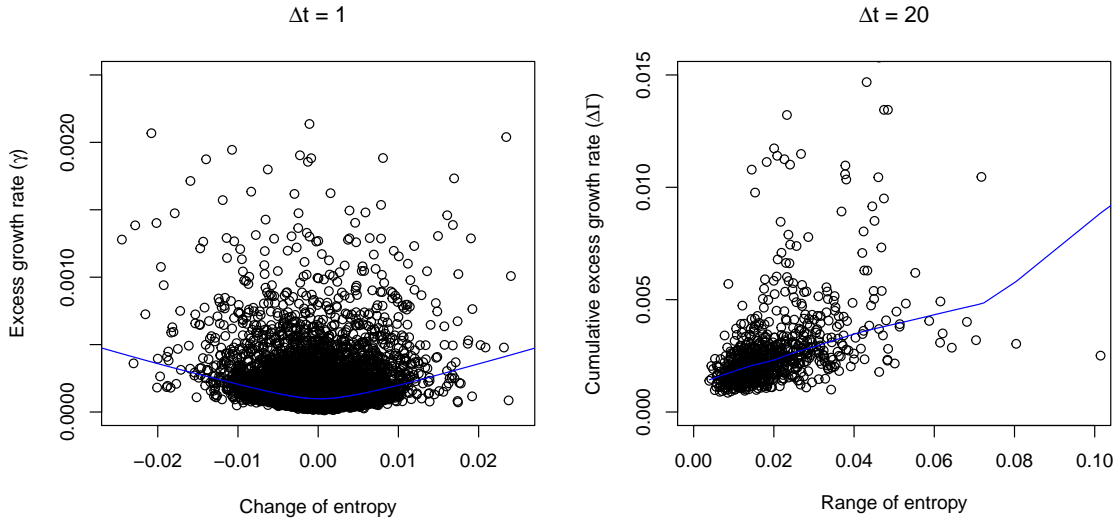


FIGURE 9. Joint behaviours of market diversity and intrinsic volatility of the largest $K = 1000$ stocks (varying over time). Left: Scatter plot of daily excess growth rate versus change of log entropy. Right: Scatter plot of cumulative (daily) excess growth rate versus range (max – min) of entropy over the same period; each point covers 20 trading days. The blue curves are fitted with locally weighted scatterplot smoothing (LOWESS). In both plots there are several outliers outside the ranges shown.

5. RANK-BASED PROPERTIES

In this section we study how the behaviours of stocks depend systematically on their relative ranks with respect to market capitalization.¹⁹ In stochastic portfolio theory there are two main motivations for the study of rank-based properties. First, as mentioned in Section 3, “projecting” to the space of ranked market capitalization or weights (thus neglecting name-based features as in the rank-based diffusion system (3.3)) allows for more parsimonious modelling of some features of market capitalizations and the capital distribution curve. Second, it is common to restrict the investment universe to a top segment of stocks by market capitalization (one reason is that these stocks are more representative of the market and are also more liquid). When strictly enforced, this means selling a stock when it drops out of the universe and buying a stock when it enters. Thus part of the turnover of the portfolio is directly related to the “intensity” of rank switching near the cut off rank.²⁰

5.1. Rank-based volatility. We first provide a quantitative illustration that smaller stocks are on average more volatile. Recall that $X_i(t)$ is the market capitalization of stock i on day t . For each rank $k \in \{1, \dots, 500\}$ we consider a *discrete quadratic variation* $QV_k(t)$ of the log market capitalization at rank k . On day t , suppose stock $i_k(t)$ has rank k . We define

$$(5.1) \quad QV_k(t+1) = QV_k(t) + (\log X_{i_k(t)}(t+1) - \log X_{i_k(t)}(t))^2,$$

¹⁹This is analogous to the practice of forming *deciles* in empirical finance: for each period, group the assets after ordering them with respect to some criterion. Here the criterion is rank (by market capitalization) and we will examine quantities indexed by rank.

²⁰Rank switching also plays an important role when the benchmark is a capitalization-weighted portfolio consisting of the largest K stocks (rather than the entire market). *Leakage* refers to the loss in wealth due to renewing the portfolio’s constituent stocks. We refer the reader to [47, Example 4.3.5] and [120] for a detailed discussion of leakage and its computation.

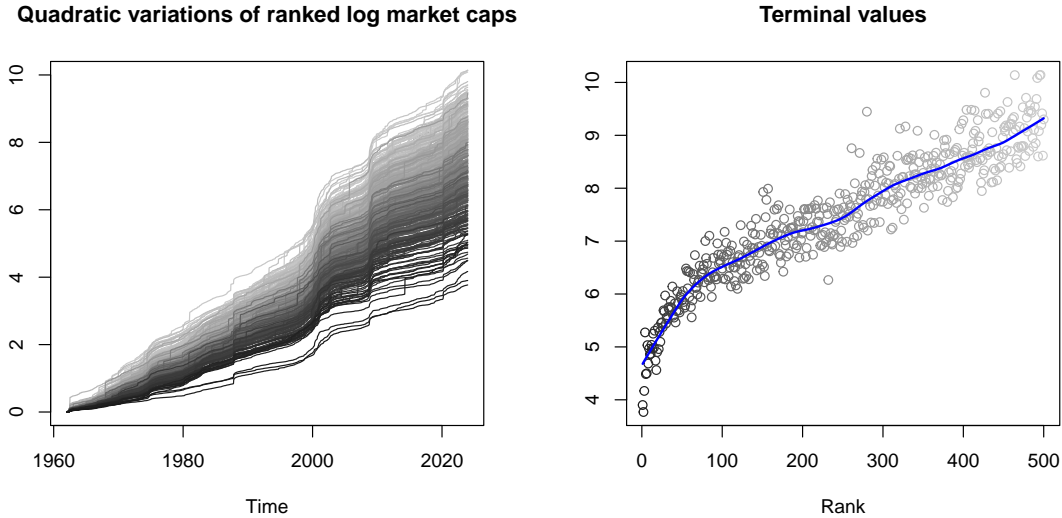


FIGURE 10. Left: Discrete quadratic variations $QV_k(t)$, defined by (5.1), for $k = 1$ (dark grey) to $k = 500$ (light grey). Right: The terminal values $QV_k(t_{\text{term}})$. Smoothed values are shown by the blue curve.

and if stock $i_k(t)$ is not traded on day $t + 1$ (e.g. delisted) we simply let $QV_k(t + 1) = QV_k$. We initialize $QV_k(t_{\text{init}}) = 0$ where t_{init} is the first trading day of the data-set. Since $i_k(t)$ varies over time, multiple stocks contribute to $QV_k(t)$ for each rank k . We show the results in Figure 10, in which the left panel plots the time series and the right panel plots the terminal values. We observe, as expected, that smaller stocks are on average more volatile and the effect is non-trivial: at the terminal time t_{term} we have $QV_{500}(t_{\text{term}}) \approx 9.33$ and $QV_1(t_{\text{term}}) \approx 4.56$.

Stylized Fact 5. *Smaller stocks are on average more volatile.*

In [18, Section 5], the first and last author analyzed further the empirical *distributions* of returns arranged by ranks. More precisely, if $R_i(t)$ is the return of stock i on day t , we define for each rank k an empirical return distribution ν_k by $\nu_k = \frac{1}{T} \sum_t \delta_{R_{i_k(t)}(t)}$, where T is the number of observations. We call $(\nu_k)_k$ a *distributional data-set* since each data point ν_k is itself a probability distribution (on \mathbb{R}). It is natural to study how the distribution ν_k varies in k . Performing geodesic principal component analysis using the *Wasserstein geometry* in optimal transport [13], we showed that smaller stocks are not only more volatile but their returns are also more positively skewed; these effects are captured by the first and second geodesic components.

5.2. Rank transition probabilities. In Figure 6 we visualize how the ranks of a collection of stocks change over time. Now we attempt a more quantitative description by estimating empirically the *transition probabilities* of daily rank transitions.

We do this straightforwardly. For each day t (over the entire sample period) and rank $k \in \{1, \dots, 1000\}$, we find the stock $i_k(t)$ at rank k . If its rank is ℓ on day $t + 1$, the *rank change* is $\ell - k$. According to our convention, a positive change in rank means that the stock becomes *relatively* smaller. For example, for $k = 2$ the possible values of rank change are $-1, 0, 1, 2, \dots$. In the case of delisting the rank change is $+\infty$. With this we obtain a matrix of relative frequencies of rank changes.²¹ The results are shown in Figure 11. As expected, we observe that rank changes are

²¹For computational purposes we consider rank changes from -50 to 50 and truncate all values beyond at the boundary values. Thus delisting means 50 in Figure 11(left) and ‘‘Increase’’ in Figure 11(right). Otherwise equal, a newly listed stock causes the ranks of all smaller stocks to increase by 1 on its first trading day.

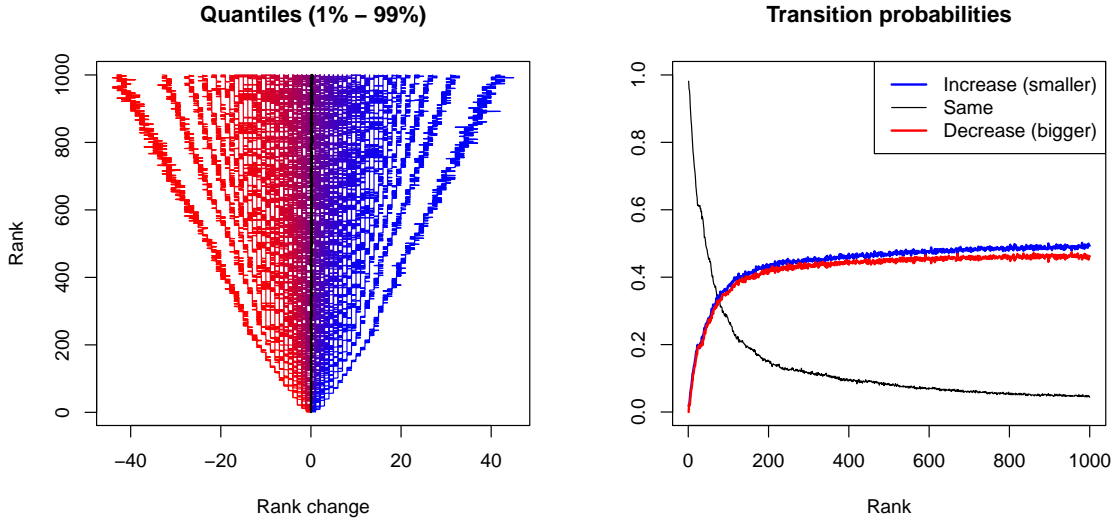


FIGURE 11. Left: Empirical distributions of daily rank changes. Shown here are the quantiles (at probabilities $0.01, 0.02, \dots, 0.99$, from blue to red) of rank change (truncated to $[-50, 50]$) at each rank from 1 to 1000. The black curve gives the mean for each rank (smoothed values range from 0.024 at rank 1 to 0.15 at rank 1000). Right: Empirical probabilities of positive (blue), null (black) and negative (red) daily rank changes as a function of rank.

statistically larger in magnitude as the rank increases. At rank 1000 the average daily rank change (after truncation and smoothing) is about 0.15; the value at rank 1 is about 0.024. These values depend on the handling of delisting. The pattern is clearer if we consider simply the *sign* (positive, zero or negative) of daily rank change, resulting in empirical probabilities $p_+(k)$, $p_0(k)$ and $p_-(k)$ for each rank k . In Figure 11(right) we observe that $p_+(k) > p_-(k)$ (with a few exceptions) and the difference $p_+(k) - p_-(k)$ increases roughly linearly as k increases. At rank 1000, the difference is (after smoothing) about 0.029, which is rather significant since the probabilities concern daily changes and cannot be accounted by IPOs and delisting alone. All effects considered, we have:

Stylized Fact 6. *There is a tendency for a stock's capitalization rank to increase (i.e., become relatively smaller).*

This finding echoes Stylized Fact 2 and highlights the importance of entrances and exits in maintaining the stability of the equity market.

5.3. Intensity of rank switching. The larger volatility of smaller stocks suggests that switching of ranks occurs more frequently among smaller stocks. To quantify this effect, we introduce an empirical quantity $\Lambda_k(t)$ which measures the (cumulative) intensity of rank switching at rank k . Its definition is motivated by a discretization of *local time* in stochastic calculus which we recall in Appendix B. We initialize each Λ_k to start at 0.

Let $Y_i(t) = \log X_i(t)$ be the log market capitalization of stock $i \in \mathcal{A}_t$ on day t , and let $Y_{(1)}(t) \geq Y_{(2)}(t) \geq \dots$ be the decreasing order statistics. Also let $i_k(t)$ be the stock which has rank k on day t . First consider the dynamics of $Y_{(1)}$. By definition, we have

$$Y_{(1)}(t+1) - Y_{(1)}(t) = Y_{(1)}(t+1) - Y_{i_k}(t) \geq Y_{i_1}(t+1) - Y_{i_1}(t).$$

Given $\Lambda_1(t)$, we define $\Lambda_1(t+1) \geq \Lambda_1(t)$ by the identity

$$(5.2) \quad Y_{(1)}(t+1) - Y_{(1)}(t) = Y_{i_1}(t+1) - Y_{i_1}(t) + \frac{1}{2}(\Lambda_1(t+1) - \Lambda_1(t)).$$

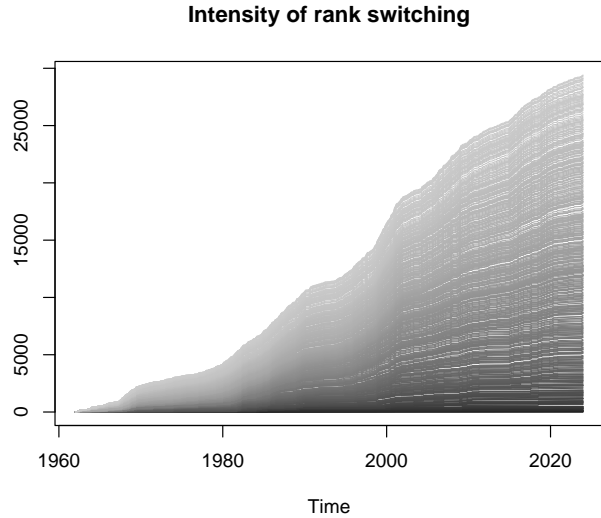


FIGURE 12. Time series of the intensity of rank switching Λ_k , from $k = 1$ (dark grey) to $k = 499$ (light grey).

Note that $\Lambda_1(t+1) = \Lambda_1(t)$ if $Y_{(1)}(t+1) = Y_{i_1(t)}(t+1)$, i.e., stock $i_k(t)$ remains the largest stock on day $t+1$. Otherwise, $\Lambda_1(t+1) - \Lambda_1(t) \geq 0$ measures the *amount of crossing*. Inductively, for each rank $k = 2, 3, \dots$, we define $\Lambda_k(t+1)$ such that

$$(5.3) \quad \begin{aligned} Y_{(k)}(t+1) - Y_{(k)}(t) &= (Y_{i_k}(t+1) - Y_{i_k}(t)) + \\ &\quad \frac{1}{2} ((\Lambda_k(t+1) - \Lambda_k(t)) - (\Lambda_{k-1}(t+1) - \Lambda_{k-1}(t))). \end{aligned}$$

(This corresponds to (B.2) in the continuous time framework.) It is not difficult to verify that $\Lambda_k(t+1) - \Lambda_k(t) \geq 0$ for all k . We call Λ_k defined by (5.2) and (5.3) the *intensity of rank switching* at rank k .²²

In Figure 12 we plot the intensity $\Lambda_k(t)$ as a function of time, for $k = 1, \dots, 499$. We observe $\Lambda_k(t)$ increases roughly linearly in time and in k . Moreover, the intensity of rank switching is very small for the largest stocks (k small). As seen in Figure 6, the largest stocks mostly remain on top and rank switches only occur occasionally. These findings are consistent with the results (concerning the period 1990–1999) presented in [47, Section 5.2].

Stylized Fact 7. *Rank switching occurs more intensely for small stocks.*

To end this section, we note that the authors of [73] constructed a rank-based volatility stabilized model and calibrated it to fit empirical behaviours of rank-based volatility, intensity of switching and some other quantities. They were also able to characterize explicitly the resulting growth optimal portfolio in their model. Further improvements of this and related models will be helpful in optimizing and backtesting trading strategies for large portfolios.

6. PERFORMANCE OF PORTFOLIOS

In this section, we show in a well-specified empirical setting that market diversity and intrinsic volatility, which are macroscopic quantities studied in the previous sections, are useful for explaining the relative performance of certain portfolios (namely, diversity-weighted portfolios with various parameters) with respect to the capitalization-weighted portfolio. Our experiment is motivated by,

²²More precisely, between rank k and rank $k+1$.

and in some aspects extends, the empirical study in [105]. In Section 6.3 we survey the literature on portfolio optimization in SPT.

6.1. Set-up of the experiment. The results of any backtesting experiment depend on many factors including market conditions during the sample period and the exact implementation of the portfolios. Here, our objective is to illustrate the effects of market diversity and intrinsic volatility in the most straightforward and hopefully convincing way.²³ In stochastic portfolio theory, these quantities arise explicitly in decompositions of portfolio performance relative to the market (see (A.8) for the case of diversity-weighted portfolio). As will be explained below, our implementation includes proportional transaction costs and handles faithfully default and delisting events. In the following, by the *support* of a portfolio at time t we mean the set $\mathcal{S}_t \subset \mathcal{A}_t$ of stocks held by the portfolio. At any given point in time our portfolios will hold at most $K = 500$ stocks.

- (i) We divide the entire sample period (1962–2023) into 62 periods corresponding to the calendar years.²⁴ The experiment is repeated independently for each *window* $[t_\ell, t_{\ell+1}]$, in the sense that for ℓ fixed, all portfolios are initiated at time t_ℓ at the same value and trade until time $t_{\ell+1}$. We refrain from maintaining portfolios over long periods since this requires specific conventions and algorithms for updating the support of the portfolio.²⁵ In the descriptions below a window $[t_\ell, t_{\ell+1}]$ is fixed.
- (ii) Our main *benchmark* portfolios are the market index tracking portfolios updated at some frequency, f . At time t_ℓ , we initialize the portfolios with the capitalization weights $w_i(t_\ell) = \mu_i^{\mathcal{A}_{t_\ell}^K}(t_\ell)$. Every f trading days these portfolios rebalance to hold the market weights of the top $K = 500$ stocks. If a stock delists in between rebalancing times, its delisting return (if provided) is treated as the last non-zero return on the security and the holding in this stock is not redistributed to other securities in the portfolio until the next rebalancing time. These portfolios are expected to behave similarly to the S&P 500, a standard benchmark portfolio for the US market, when $[t_\ell, t_{\ell+1}]$ is reasonably short.
- (iii) We backtest *diversity-weighted portfolios* $w^{p,f}$ (see also A.7) parameterized by $p \in [0, 1]$ and a rebalancing frequency $f \in \{1, 2, \dots\} \cup \{\infty\}$. It is initialized at t_ℓ to have weights

$$w_i^{p,f}(t_\ell) = \frac{\left(\mu_i^{\mathcal{A}_{t_\ell}^K}(t_\ell)\right)^p}{\sum_{j \in \mathcal{A}_{t_\ell}^K} \left(\mu_j^{\mathcal{A}_{t_\ell}^K}(t_\ell)\right)^p}, \quad i \in \mathcal{A}_{t_\ell}^K.$$

The diversity-weighted portfolio, introduced in [50, 53], is a key example of *functionally generated portfolio* in SPT, where the portfolio weights are deterministic functions of the market weights. Note that the portfolio is equal-weighted²⁶ when $p = 0$ and capitalization-weighted when $p = 1$, so we may regard p as an interpolation parameter. These portfolios are frequently used in empirical studies, see e.g. [90, 101, 107, 123]. The portfolio then rebalances and reinvests dividends (and cash proceeds from delistings) every f trading days

²³The codes of our implementation are available at our Github repository and the reader is invited to vary the settings.

²⁴This frequency is chosen so that we may illustrate performance in a variety of market conditions. Moreover, the top segment \mathcal{A}_t^K does not change drastically over $[t_\ell, t_{\ell+1}]$.

²⁵Development of systematic methods is an interesting direction but is beyond the scope of this paper.

²⁶An equal-weighted portfolio may be used as another benchmark. For example, the S&P 500 Equal Weight Index is the equal-weighted version of the usual S&P 500. In [100], the author argued that under suitable conditions, the equal-weighted portfolio approximates the numéraire portfolio as the number of securities tends to infinity.

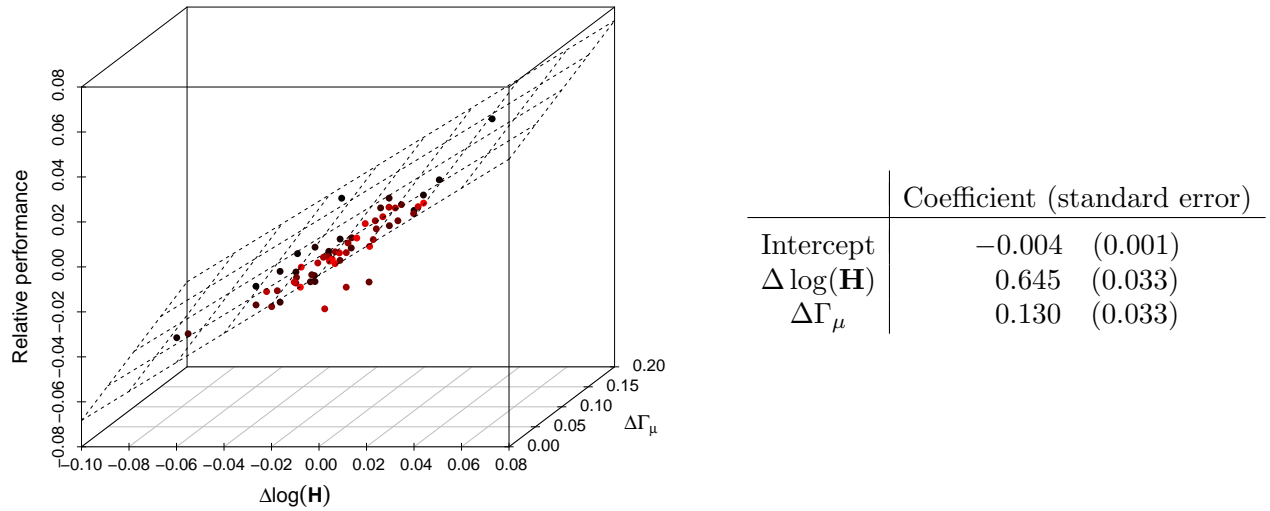


FIGURE 13. Illustration of the linear regression (6.1) concerning the annual relative performance of the equal-weight portfolio to the market index tracking portfolio, $\Delta \log(Z_{0,10}/Z_{1,10})$. Left: Scatter plot of the data with the fitted surface. Right: Regression coefficients $\hat{\beta}_i$ and standard errors (from ordinary least squares).

to the weights

$$w_i^{p,f}(t) = \frac{(\mu_i^{\mathcal{S}_t}(t))^p}{\sum_{j \in \mathcal{S}_t} (\mu_j^{\mathcal{S}_t}(t))^p}, \quad i \in \mathcal{S}_t := \mathcal{A}_t^K,$$

while paying proportional transaction costs. Note that by construction $w^{1,f}$ are the benchmarks in (ii). In Section 6.2 we will report results for $p \in \{0, 0.01, \dots, 1\}$ and $f \in \{1, 2, 5, 10, 25, 50, 125, \infty\}$. We let $Z_{p,f}(t)$ be the wealth of the portfolio $w^{p,f}$, normalized to 1000 at time t_ℓ .

(iv) In (ii) and (iii), all trading activities (except initialization) incur *proportional transaction costs* following exactly the procedure described in [105, Section 2.1]. In view of [18, 105], we choose a cost of 0.25% for all stocks on purchases and sales. The empirical study [5] and the NASDAQ report [89] also support a choice of cost on this order of magnitude.

6.2. Empirical results.

6.2.1. *Effect of diversity and intrinsic volatility in relative performance.* The above set-up yields, for each window $[t_\ell, t_{\ell+1}]$, a wealth process for each portfolio $w^{p,f}$, $p \in [0, 1]$ and $f \in \{1, \dots\}$. To underscore the relevance of diversity and intrinsic volatility in explaining the relative performance of portfolios, we regress the annual performance of the equal weight portfolio $w^{0,10}$ relative to the capitalization-weighted portfolio $w^{1,10}$ (both rebalanced every 10 days) against the annual changes in entropy and the (cumulative) *daily* market excess growth rate (of \mathcal{A}_t^K for both quantities). Explicitly, we fit by ordinary least squares the linear model

$$(6.1) \quad \Delta \log(Z_{0,10}(t_\ell)/Z_{1,10}(t_\ell)) \sim \beta_0 + \beta_1 \Delta \log \mathbf{H}(\mu_i^{\mathcal{A}_{t_\ell}^K}(t_\ell)) + \beta_2 \Delta \Gamma_\mu(t_\ell),$$

where Δ is the forward difference operator, $\Delta Z(t_\ell) = Z(t_{\ell+1}) - Z(t_\ell)$. We illustrate the fit in Figure 13 (left) and report the estimated coefficients in Figure 13 (right). The R^2 and Adjusted R^2 values for the calibrated model are 0.87 and 0.86, respectively.

Under an idealized theoretical set-up in stochastic portfolio theory (see Appendix A), a portfolio relative value decomposition reminiscent of the model in (6.1) should hold.²⁷ This theoretical decomposition does not hold exactly in practice since our data comes from trading subject to transaction costs in a market with dividends, defaults, and a changing set of constituent securities. Nevertheless, the model we posit in (6.1) does an excellent job of explaining relative performance. The estimated values of β_1 and β_2 are positive, meaning the rebalanced portfolio benefits from a positive change in market diversity and large intrinsic volatility. From the values of these coefficients (and the typical magnitudes of $\Delta \log \mathbf{H}$ and $\Delta \Gamma_\mu$), we also observe that over a short horizon (say a year), a change in market diversity has a larger impact on relative performance than intrinsic volatility. The estimated value of β_0 is negative; this can be attributed to the increase in transaction costs (relative to the benchmark). Moreover, modulo changes to the estimated coefficients, these conclusions are robust to variations in parameters of the portfolio $w^{p,f}$ and benchmark $w^{1,f}$ which underscores the conceptual importance of these explanatory variables.

6.2.2. Sensitivity to portfolio specifications. Building off of the analysis in Figure 13, we can investigate the range of performance that was realised historically by the portfolios $w^{p,f}$. Figure 14 illustrates the annual performance accessible by varying p and f side-by-side with the explanatory variables from (6.1).

The top left panel of Figure 14 illustrates the annual performance of the (approximately) monthly rebalanced diversity p portfolio, $w^{p,20}$, relative to the index tracking benchmark updated at the same frequency, $w^{1,20}$. Each year has a bar which spans the range of performance for values $p \in [0, 1]$. The relative performance of a fixed p is given by the color gradient in the bar which goes from black to white as p increases from 0 to 1. By definition, when $p = 1$ the relative performance is 0. In most years, the over/under-performance of the portfolio $w^{p,20}$ is monotone in p as underscored by the monotone change in the bars from black to white. The bottom left panel illustrates the change in entropy over the same calendar years and allows us to compare the performance statistics. It is visually apparent that the directional change in entropy tracks with the orientation of the bars in the top left panel. When entropy increases, smaller values of p tend to outperform and vice-versa.

The top right panel of Figure 14 plots the annual performance of the equal weight portfolio $w^{0,f}$ relative to the buy-and-hold (initially equal-weighted) portfolio $w^{0,\infty}$ for various *fixed* rebalancing frequencies, f . Since there are approximately 250 trading days every year, we choose the set of divisors $\{1, 2, 5, 10, 25, 50, 125, \infty\}$ ²⁸. The range of the gray bars represents the relative performance spanned by the portfolios in this set. Once again, by construction, when $f = \infty$ the relative performance is 0. Within each of the bars we mark the value corresponding to a given f by a colored line that changes on a gradient from blue to red as f increases. Unlike the top left panel, the relationship here is not monotone in general. There are many years when intermediate values of f outperform. We see that, for most years, the choice of frequency is less material than the choice of p in determining the degree of over/under-performance. That said, we observe that frequent rebalancing (say, every 1–2 days) underperforms in most years under 0.25% transaction cost. Also, around the financial crises of 2000 and 2008 the right rebalancing decision appears to meaningfully impact portfolio returns. The bottom right panel displays the difference in the cumulative daily excess growth rate and the annual excess growth rate for the calendar years in our backtest. This statistic captures the difference in the intrinsic volatility at these two different rebalancing scales. However, we see that this only has a weak positive relationship with the difference in performance

²⁷In the regression, we use entropy and market excess growth rate (rather than the quantities on the right hand side of (A.8)) since they were discussed in depth in previous sections and already give good fit.

²⁸If a year has 250 trading days then $f = \infty$ will give the same result as any $f > 250$.

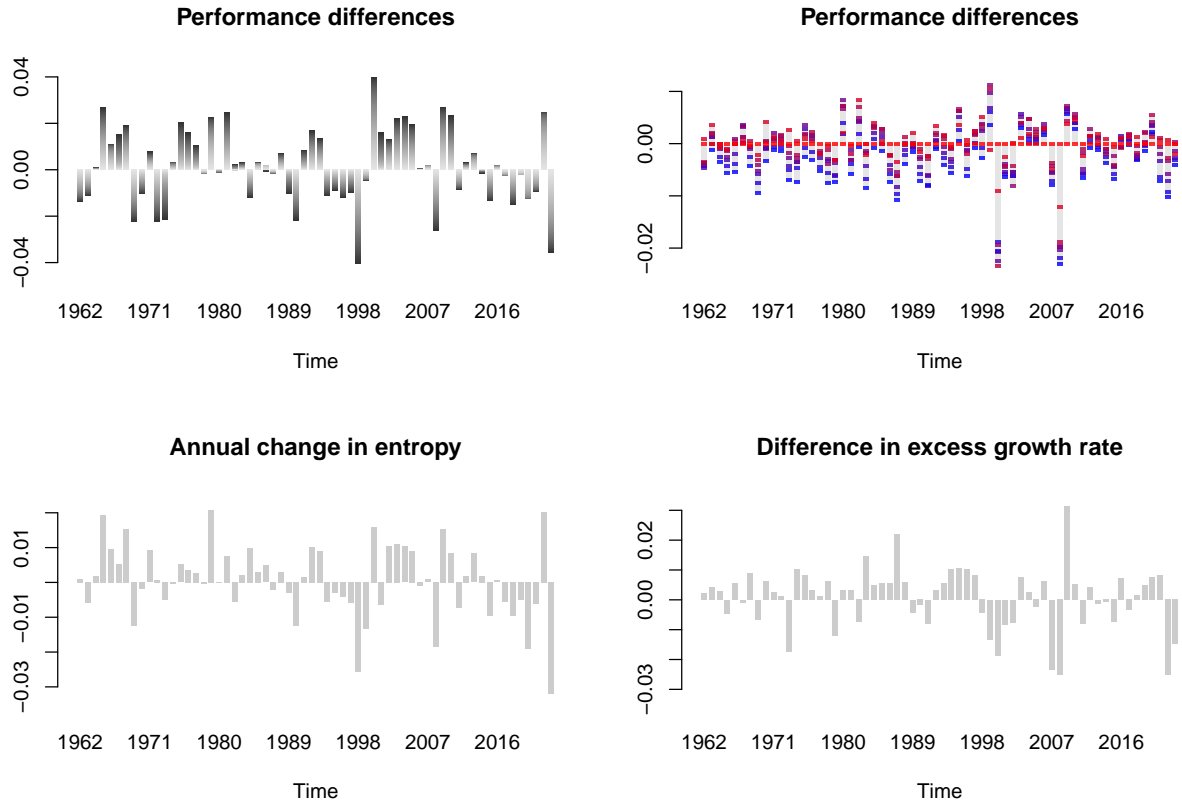


FIGURE 14. Top Left: Bar plot of $\Delta \log(Z_{p,20}/Z_{1,20})$ for each year on a gradient from black to white as p ranges from 0 to 1. Bottom Left: Annual change in entropy, $\Delta \log(\mathbf{H})$. Top Right: Bar plot of $\Delta \log(Z_{0,f}/Z_{0,\infty})$ for each year. The gray bar represents the full range of performance associated with frequencies $f \in \{1, 2, 5, 10, 25, 50, 125, \infty\}$. Solid lines ranging from blue to red mark the performance corresponding to a particular f as the values increase. Bottom Right: Annual change in the cumulative daily excess growth rate $\Delta \Gamma_\mu$ (i.e. $\Delta t = 1$ in Figure 7 (left)) less the annual excess growth rate γ_μ (4.1) for the same period.

due to changes in f . This is not unexpected, since the contribution of the excess growth rate to portfolio returns is a second order effect (see, e.g. Figure 13) and the strength of the relationship can be confounded by many other market factors including transaction costs, defaults, and a variable set of constituent securities.

6.2.3. Sharpe ratio and drawdown. To date, relatively little has been studied about portfolio risks and risk adjusted returns in the context of stochastic portfolio theory. In their empirical analysis, [105] reported the historical Sharpe ratios of several SPT portfolios and illustrated an approximately linear decay in increasing transaction costs. There has also been some related theoretical work on drawdown constrained growth rate optimization (see [36] and [77, Section 4.1]). The first and last author proposed in [19] an optimization framework that allows flexibility in the exposure to market diversity. In view of this gap in the literature, we take the opportunity to investigate the risk profile of the diversity-weighted portfolios $w^{p,f}$ that have been the subject of our empirical investigation.

Figure 15 presents two scatter plots for the risk statistics of the (approximately) monthly rebalanced diversity portfolios $w^{p,20}$. The left panel plots the (maximum) drawdown and Sharpe ratio (of the daily returns) in each calendar year for the portfolios. The right panel compares the

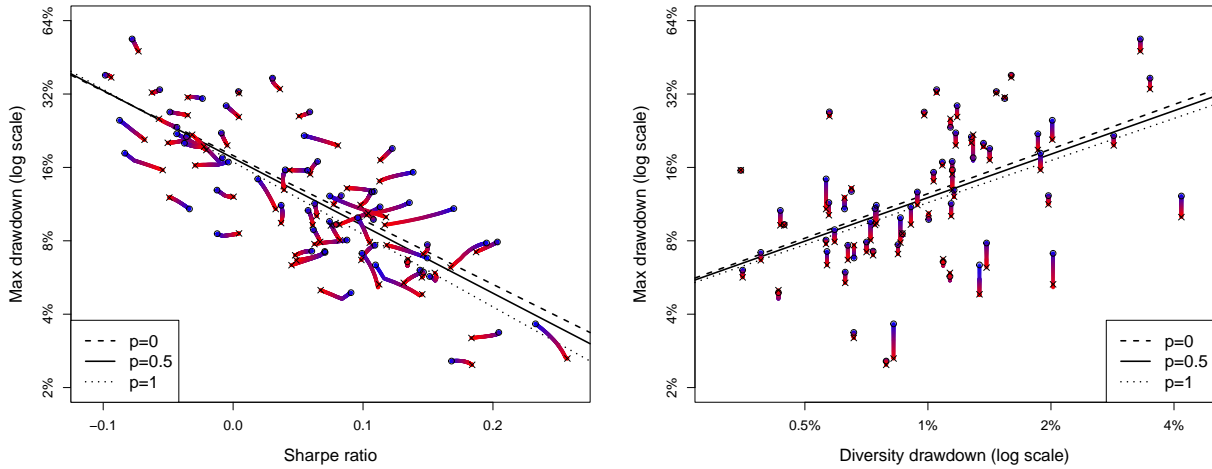


FIGURE 15. Scatter plots for the risk statistics of the portfolio $w^{p,20}$ (roughly monthly rebalanced). Each point corresponds to a year from 1962 to 2023 on color gradient from blue to red as p ranges from 0 to 1. The values corresponding to $p = 0$ and $p = 1$ are emphasized with the symbols \circ and \times , respectively. Left: Annual portfolio drawdown against its Sharpe ratio. Right: Annual portfolio drawdown against the drawdown of market diversity in the same period. In both plots there are lines from a least squares fit of the data for $p \in \{0, 0.5, 1\}$.

portfolio drawdown to the drawdown of diversity/market entropy. In both plots, the points are drawn with a color gradient that goes from blue to red as p is varied from 0 to 1. The overall relationship is emphasized in each plot with a regression line corresponding to the data for portfolios with $p \in \{0, 0.5, 1\}$. In general, we see that years with a higher Sharpe ratio tend to have a lower drawdown, and that drawdowns in diversity are positively correlated with drawdowns in portfolio value. We emphasize here that all the portfolio statistics are in terms of the *absolute* returns, and not the *relative* returns (with respect to the market). This explains the order of magnitude difference in the statistics for the diversity and portfolio drawdown (by comparison, see the relative performance values in Figure 13). While the general trend is consistent, we can see that the Sharpe ratio and drawdown in a given year can behave non-linearly in p . In both scatter plots we also observe years where the choice of p is relatively immaterial to the final risk statistic, and times where there is a large range of values. Overall, as p increases the average drawdown decreases slightly and the portfolio is slightly less sensitive to drawdowns in diversity. This is to be expected since lower values of p overweight the smallest stocks and tend to have a higher turnover (relative to the index tracking portfolio) which makes them more “aggressive”.

6.3. Portfolio optimization in SPT. Although we do not address the optimization of large equity portfolios in this paper, we do attempt to briefly survey existing work in this direction. The present literature within SPT can be placed roughly into three groups according to their focus on theory or applications. The largest body of work in this area is theoretical, with the earliest works in SPT focusing on the optimization of outperformance/arbitrage relative to the market [44, 45, 46]. Subsequently, several authors have studied in depth the robust optimization of long run portfolio growth [11, 71, 72, 74, 81, 82]. Optimization of functionally generated portfolios in discrete time was considered in [117] and the works [35, 118] extended Cover’s universal portfolio [29] to the setting of SPT, and studied its asymptotic optimality. On the data-driven side, there have been investigations on methods to improve returns by dynamically switching to the market portfolio

[111] and machine learning approaches to portfolio optimization [107]. Living somewhere in the middle, the papers [19, 34] present theory related to classes of portfolio optimization problems, and validate their performance using historical financial data. Specifically, the paper [19] studies a non-parametric optimization problem over a special family of rank-based functionally generated portfolios, while [34] studies the optimization of linear path-functional portfolios which they prove have a universal approximation property.

7. CONCLUSION

In this paper, we conducted a systematic empirical study of several macroscopic properties of the US equity market using the CRSP Database. In the process, we illustrated and highlighted several stylized facts, both old and new. Of particular interest is the apparent importance of entrances and exits in producing a stable market ecosystem. Throughout our analysis we have made a concerted effort to suggest novel research directions motivated by stochastic portfolio theory and our findings, and to point to related work that we are aware of where applicable. All of our analysis can be replicated by the code from our repository and we encourage interested readers to interact with the study. In particular, the backtesting engine provided therein may be of independent interest to researchers and practitioners. Apart from the problems discussed throughout the paper, we highlight the following directions for further investigation:

- (i) (Other markets) Most empirical studies in stochastic portfolio theory considered the US equity market largely thanks to the convenient CRSP Database. It is interesting to see to what extent the stylized facts we discussed extend to other equity markets in the past and the present. Also, one may consider several markets (e.g. all Asian markets) as a whole. While we expect many properties (such as the stability of the capital distribution curve and the intensity of rank switching) are common across markets, there are also important differences. To give an example, consider the *MSCI Korea Index* [1] which covers about 85% of the Korean equity universe. As of July 2024, the biggest company, Samsung Electronics, covers alone over 30% of the index. In this sense, the Korean market is much more concentrated than the US market.²⁹
- (ii) (Other quantities and intraday data) In this paper we focused on macroscopic properties defined in terms of market capitalizations and returns. Other quantities, such as trading volumes, signatures (in the sense of rough path theory) [32], sectors, prices of options³⁰ and exchange traded funds, may offer additional insights. Also, the CRSP Database offers daily but not intraday data. SPT-inspired analysis of high frequency data is promising but largely open; the only work we are aware of is [57] which studied intraday properties of the excess growth rate in relation to the profits made by market makers. A possible direction is to study intraday return distributions (see e.g. [121]) and relate them with market capitalizations and other quantities.
- (iii) (Adaptive portfolio selection under realistic conditions) Our empirical study and the back-test conducted in Section 6 naturally suggest the study of systematic approaches for portfolio selection with a large but evolving number of assets and under transaction costs. Short positions, derivatives, and adaptive rebalancing frequencies may also be considered. Needless to say, these and other issues are involved in all actual portfolios but are not easy to incorporate in theoretical models in mathematical finance. We hope our work serves as a bridge between the theoretical and practical sides.

²⁹For comparison, we note that as of July 2024, the largest three stocks in S&P 500 are Microsoft (7.0%), Apple (6.9%) and Nvidia (6.2%).

³⁰See [60] for some relationships between contingent claims and functionally generated portfolios in SPT.

ACKNOWLEDGEMENT

S. Campbell and T.-K. L. Wong thank Martin Larsson, David Itkin and Robert Jones for helpful discussions. The research of T.-K. L. Wong is partially supported by an NSERC Discovery Grant (RGPIN-2019-04419) and a Seed Funding for Methodologists Grant from the Data Sciences Institute (DSI) at the University of Toronto. The authors report there are no competing interests to declare.

APPENDIX

APPENDIX A. CRASH COURSE IN STOCHASTIC PORTFOLIO THEORY

We provide an overview of some basic concepts of *stochastic portfolio theory* (SPT). Our aim is to describe an idealized market model and use it to motivate some of the topics discussed in the main text. Systematic introductions to SPT can be found in standard references of the subject such as [47, 56] (also see [77]). We also refer the reader to [97, 119] for a discrete time formulation which does not require stochastic calculus. Another model-free approach using *rough paths* in continuous time is developed in [3].

Consider an equity market model consisting of a *fixed* collection of n non-dividend paying stocks.³¹ The market capitalizations $X_1(t), \dots, X_n(t)$ of the stocks are modelled as a vector of positive Itô processes defined on some filtered probability space. The vector $\mu(t) = (\mu_1(t), \dots, \mu_n(t))$ of market weights, where $\mu_i(t) = X_i(t)/(X_1(t) + \dots + X_n(t))$, takes values in the open unit simplex Δ_n . The *diversity* of the market refers to the concentration of the capital distribution, and may be quantified in terms of a symmetric concave function $\Phi : \Delta_n \rightarrow (0, \infty)$ (see [47, Section 3.4]). Popular choices include the *Shannon entropy* $\mathbf{H}(\mu)$ (see (3.4)) as well as the parameterized diversity $\mathbf{D}_p(\mu)$ (see (3.5)). It was observed empirically that market diversity tends to “mean-reverting” in the long run (see Section 3.2). At the very least, the market weight vector $\mu(t)$ tends to avoid certain regions of the simplex especially its vertices. Motivated by this and other empirical observations, various *path properties* may be imposed on the market model. For example, the market is said to be *coherent* if a.s. $\lim_{t \rightarrow \infty} \frac{1}{t} \log \mu_i(t) = 0$ for all i , and is *diverse* if there exists $\delta > 0$ such that a.s. $\max_{1 \leq i \leq n} \mu_i(t) \leq 1 - \delta$ for all i and $t \geq 0$. Note that some conditions, when imposed to hold with probability 1, exclude the existence of an equivalent martingale measure (over a finite horizon); see [56, Section 6] for a discussion.

An *all-long self-financing portfolio* is represented by a progressively measurable process $\pi(t) = (\pi_1(t), \dots, \pi_n(t))$ with values in the closure of Δ_n . We interpret $\pi_i(t)$ as the percentage of current capital invested in stock i . Henceforth all portfolios are assumed to be all-long and self-financed. In SPT, we focus on the *relative value* $V_\pi(t)$ of the portfolio with respect to the market portfolio. This amounts to taking the value $X_1(t) + \dots + X_n(t)$ of the market portfolio as the numeraire. Assuming frictionless continuous trading, the relative value satisfies $\frac{dV_\pi(t)}{V_\pi(t)} = \sum_{i=1}^n \pi_i(t) \frac{d\mu_i(t)}{\mu_i(t)}$. By Itô’s formula, we have

$$(A.1) \quad d \log V_\pi(t) = \sum_{i=1}^n \pi_i(t) d \log \mu_i(t) + d\Gamma_\pi(t),$$

where $\Gamma_\pi(t)$ is a non-decreasing finite variation process called the *cumulative excess growth rate* of the portfolio. It is given by

$$(A.2) \quad d\Gamma_\pi(t) = \frac{1}{2} \left(\sum_{i=1}^n \pi_i(t) d\langle \log \mu_i \rangle(t) - \sum_{i,j=1}^n \pi_i(t) \pi_j(t) d\langle \log \mu_i, \log \mu_j \rangle(t) \right),$$

³¹Dividends are included in Fernholz’s original market model [47] but are frequently omitted for convenience. See [12, 78] for recent attempts to relax the assumption of a fixed investment universe.

where $\langle \cdot \rangle$ denotes quadratic (co)variation. Its increments can be approximated by the (discrete) *excess growth rate* (see Section 4): for $\Delta t > 0$ small we have

$$(A.3) \quad \Gamma_\pi(t + \Delta t) - \Gamma_\pi(t) \approx \log \left(\sum_{i=1}^n \pi_i(t) \frac{\mu_i(t + \Delta t)}{\mu_i(t)} \right) - \sum_{i=1}^n \pi_i(t) \log \frac{\mu_i(t + \Delta t)}{\mu_i(t)}.$$

The cumulative excess growth rate $\Gamma_\mu(t)$ of the *market portfolio* $\pi \equiv \mu$ is especially important and may be regarded as a measure of the *intrinsic* (or *relative*) *volatility* of the market. This concept decouples the absolute volatility of the market with the relative volatility among the constituent stocks. For the market portfolio, (A.2) simplifies and yields

$$(A.4) \quad d\Gamma_\mu(t) = \frac{1}{2} \sum_{i=1}^n \mu_i(t) d\langle \log \mu_i \rangle(t) = \frac{1}{2} \sum_{i=1}^n \frac{d\langle \mu_i \rangle(t)}{\mu_i(t)}.$$

In fact, $\Gamma_\mu^*(t)$ is ($\frac{1}{2}$ times) the Riemannian quadratic variation of the simplex-valued continuous semimartingale $\mu(\cdot)$ if we equip Δ_n with the *Fisher-Rao Riemannian metric* (see [4, 41] for the precise definitions).

A portfolio π is said to be a *relative arbitrage* with respect to the market portfolio over a finite horizon $[0, T]$, if

$$(A.5) \quad \mathbb{P}(V_\pi(T) \geq V_\pi(0)) = 1 \quad \text{and} \quad \mathbb{P}(V_\pi(T) > V_\pi(0)) > 0.$$

A key insight of SPT is that relative arbitrages exist under fairly realistic conditions which do not fully specify the market model. In this sense SPT is partially *model-free*.

To illustrate this idea, consider first a *constant-weighted portfolio* $\pi(t) \equiv \pi \in \Delta_n$. From (A.1), the relative growth rate of the portfolio satisfies

$$(A.6) \quad \frac{1}{t} \log \frac{V_\pi(t)}{V_\pi(0)} = \sum_{i=1}^n \frac{1}{t} \pi_i \log \frac{\mu_i(t)}{\mu_i(0)} + \frac{1}{t} \Gamma_\pi(t).$$

If the market is coherent, the first term on the right hand side of (A.6) tends to 0 as $t \rightarrow \infty$. Suppose further that the market is diverse and is *nondegenerate* in the sense that the covariance process of $\log X(t)$ is uniformly elliptic [47, Definition 1.1.2]. Then, it can be shown that $d\Gamma_\pi(t) \geq \epsilon dt$ for some constant $\epsilon > 0$. Letting $t \rightarrow \infty$ in (A.6), we have $\liminf_{t \rightarrow \infty} \frac{1}{t} \log \frac{V_\pi(t)}{V_\pi(0)} \geq \epsilon$ a.s., thus giving an “asymptotic relative arbitrage”.

To give an explicit example of relative arbitrage in the sense of (A.5), consider the *diversity-weighted portfolio* which is closely related to the function \mathbf{D}_p in (3.5) and is given by

$$(A.7) \quad \pi_i(t) = \frac{\mu_i^p(t)}{\sum_{j=1}^n \mu_j^p(t)}, \quad i = 1, \dots, n,$$

where $p \in (0, 1)$ is a tuning parameter. Note that letting $p \rightarrow 0$ recovers the equal-weighted portfolio $\pi_i(t) \equiv \frac{1}{n}$ and letting $p \rightarrow 1$ recovers the market portfolio $\pi(t) \equiv \mu(t)$. Using Itô’s formula, one can show that the relative value of the portfolio satisfies the *pathwise decomposition*

$$(A.8) \quad \log \frac{V_\pi(t)}{V_\pi(0)} = \log \frac{\mathbf{D}_p(\mu(t))}{\mathbf{D}_p(\mu(0))} + (1 - p)\Gamma_\pi(t), \quad t \geq 0.$$

From (A.7), the relative performance of the portfolio is characterized by (i) the change in market diversity and (ii) market volatility measured by the excess growth rate of the portfolio. The excess growth rate contributes positively to relative performance, but over the short run the dynamics of $\log V_\pi(t)$ is dominated by that of $\log \mathbf{D}_p(\mu(t))$. As the parameter p varies between 0 and 1, we have a trade-off between exposure to intrinsic volatility versus diversity.³² Assume that the market is

³²See [114] for an analysis of the diversity-weighted portfolio when p is *negative*.

diverse, so that $\log \mathbf{D}_p(\mu(t)) \geq -M$ for some $M > 0$. If the market is also nondegenerate, then $d(1-p)\Gamma_\pi(t) \geq \epsilon dt$ for some $\epsilon > 0$. This gives the a.s. lower bound

$$\log \frac{V_\pi(t)}{V_\pi(0)} \geq -M - \log \mathbf{D}_p(\mu(0)) + \epsilon t, \quad t \geq 0,$$

and we have a relative arbitrage over $[0, T]$ whenever $T > T^* := \frac{1}{\epsilon}(M + \log \mathbf{D}_p(\mu(0)))$ (unfortunately, the bound T^* obtained this way is too large for practical purposes). Both the constant-weighted portfolio and the diversity-weighted portfolio are special cases of *functionally generated portfolios* for which a pathwise decomposition analogous to (A.7) holds.³³ Relative arbitrages can also be constructed over short time horizons or under weaker conditions. For further details and more recent developments, we refer the reader to [3, 19, 48, 78, 97] and the references therein.

APPENDIX B. LOCAL TIME

We recall the concept of *local time* in stochastic calculus which motivates the development in Section 5.3 and is closely related to the concept of leakage in stochastic portfolio theory. We follow the notations of [47, Section 4.1]. Further details can be found in [103, Chapter VI], [9] and [120]. Let $Y(t)$ be a real-valued continuous semimartingale defined on a filtered probability space. The *local time* of Y at 0 is the non-decreasing process Λ defined by the identity

$$(B.1) \quad \frac{1}{2}|Y(t)| = \frac{1}{2}|Y(0)| + \frac{1}{2} \int_0^t \text{sign}(Y(s))dY(s) + \Lambda(t),$$

where $\text{sign}(y) = 1$ if $y > 0$ and $\text{sign}(y) = -1$ if $y \leq 0$. We may regard (B.1) as an extension of Itô's formula applied to the convex function $y \mapsto \frac{1}{2}|y|$ whose distributional second derivative is a point mass at 0. It can be shown that $d\Lambda(t) = 0$ on $\{t : Y(t) \neq 0\}$. Intuitively, $\Lambda(t)$ characterizes the “amount of time” Y spends at the point 0 (this is justified by the *occupation formula* which involves the local time at each $y \in \mathbb{R}$).

Next consider an n -dimensional continuous semimartingale (Y_1, \dots, Y_n) . We say that Y_1, \dots, Y_n are *pathwise mutually non-degenerate* if:

- (i) for all $i \neq j$, $\{t : Y_i(t) = Y_j(t)\}$ has Lebesgue measure zero a.s.;
- (ii) (triple collision) for all $i < j < k$, $\{t : Y_i(t) = Y_j(t) = Y_k(t)\} = \emptyset$ a.s.

Write $Y_i(t) = Y_i(0) + M_i(t) + A_i(t)$ where M_i is the local martingale part and A_i has finite variation. We say that Y_i is *absolutely continuous* if the random signed measures A_i and $\langle M \rangle_i$ are a.s. absolutely continuous with respect to the Lebesgue measure. Let $Y_{(1)}(t) \geq \dots \geq Y_{(n)}(t)$ be the non-increasing order statistics of $Y_1(t), \dots, Y_n(t)$. We are interested in the *gaps* $Y_{(1)} - Y_{(2)}, \dots, Y_{(n-1)} - Y_{(n)}$ which are non-negative by construction. Since Y is continuous, if a rank switch between ranks k and $k+1$ occurs at t then $Y_{(k)}(t) - Y_{(k+1)}(t) = 0$. Thus we may use the local time of $Y_{(k)} - Y_{(k+1)}$ at 0 to measure to intensity of rank switching.

Proposition 8. [47, Proposition 4.1.11] *Let Y_1, \dots, Y_n be pathwise mutually non-degenerate and absolutely continuous. Then $(Y_{(1)}, \dots, Y_{(n)})$ is an n -dimensional continuous semimartingale. For $k = 1, \dots, n-1$, let $\Lambda_k(t)$ be the local time of the non-negative semimartingale $Y_{(k)} - Y_{(k+1)}$ at 0. Also let $\Lambda_0(t) = \Lambda_{n+1}(t) = 0$. Then*

$$(B.2) \quad dY_{(k)}(t) = \sum_{i=1}^n \mathbf{1}_{\{Y_i(t)=Y_{(k)}(t)\}} dY_i(t) + \frac{1}{2} (d\Lambda_k(t) - d\Lambda_{k-1}(t)).$$

³³Analogous pathwise decompositions can be established without a stochastic model. See [97] for the discrete time case and [3] for the continuous time case using rough path theory. For generalizations of functional portfolio generalization see [79, 83, 119] and the references therein.

This result enables one to recover the local times of the gaps $Y_{(k)} - Y_{(k+1)}$ from the ranked processes $Y_{(k)}(t)$ and stochastic integrals of the form $\sum_i \mathbf{1}_{\{Y_i(t)=Y_{(k)}(t)\}} dY_i(t)$. In the context of Section 5.3, $Y_i(t) = \log X_i(t)$ is the log market capitalization of stock i .

REFERENCES

- [1] MSCI Korea Index (KRW). <https://www.msci.com/documents/10199/2dae4ac7-240b-42a7-87be-1cac61d547eb>. Accessed: 2024-08-26.
- [2] A. Agapova, R. Ferguson, and J. Greene. Market diversity and the performance of actively managed portfolios. *The Journal of Portfolio Management*, 38(1):48–59, 2011.
- [3] A. L. Allan, C. Cuchiero, C. Liu, and D. J. Prömel. Model-free portfolio theory: A rough path approach. *Mathematical Finance*, 33(3):709–765, 2023.
- [4] S.-i. Amari. *Information Geometry and Its Applications*. Springer, 2016.
- [5] A. Anand, A. Puckett, P. Irvine, and K. Venkataaraman. Market crashes and institutional trading: Evidence from us equities during the financial crisis of 2007-08. *Journal of Financial Economics*, 108:773–797, 2013.
- [6] F. Audrino, R. Fernholz, and R. G. Ferretti. A forecasting model for stock market diversity. *Annals of Finance*, 3(2):213–240, 2007.
- [7] T. G. Bali, R. F. Engle, and S. Murray. *Empirical Asset Pricing: The Cross Section of Stock Returns*. John Wiley & Sons, 2016.
- [8] A. D. Banner, R. Fernholz, and I. Karatzas. Atlas models of equity markets. *The Annals of Applied Probability*, 15(4):2296–2330, 2005.
- [9] A. D. Banner and R. Ghomrasni. Local times of ranked continuous semimartingales. *Stochastic Processes and their Applications*, 118(7):1244–1253, 2008.
- [10] R. F. Bass and E. Pardoux. Uniqueness for diffusions with piecewise constant coefficients. *Probability Theory and Related Fields*, 76(4):557–572, 1987.
- [11] E. Bayraktar and Y.-J. Huang. Robust maximization of asymptotic growth under covariance uncertainty. *The Annals of Applied Probability*, pages 1817–1840, 2013.
- [12] E. Bayraktar, D. Kim, and A. Tilva. Quantifying dimensional change in stochastic portfolio theory. *Mathematical Finance*, 2023.
- [13] J. Bigot, R. Gouet, T. Klein, and A. López. Geodesic PCA in the Wasserstein space by convex PCA. *Annales de l'Institut Henri Poincaré, Probabilités et Statistiques*, 53(1):1–26, 2017.
- [14] L. Blume and D. Easley. Evolution and market behavior. *Journal of Economic theory*, 58(1):9–40, 1992.
- [15] D. G. Booth and E. F. Fama. Diversification returns and asset contributions. *Financial Analysts Journal*, 48(3):26–32, 1992.
- [16] P. Bouchey, V. Nemtchinov, and T.-K. L. Wong. Volatility harvesting in theory and practice. *The Journal of Wealth Management*, 18(3):89, 2015.
- [17] J. Y. Campbell, A. W. Lo, and A. C. MacKinlay. *The Econometrics of Financial Markets*. Princeton University Press, 1997.
- [18] S. Campbell and T.-K. L. Wong. Efficient Convex PCA with applications to Wasserstein geodesic PCA and ranked data. *arXiv preprint arXiv:2211.02990*, 2022.
- [19] S. Campbell and T.-K. L. Wong. Functional portfolio optimization in stochastic portfolio theory. *SIAM Journal on Financial Mathematics*, 13(2):576–618, 2022.
- [20] N. A. Canakgoz and J. E. Beasley. Mixed-integer programming approaches for index tracking and enhanced indexation. *European journal of operational research*, 196(1):384–399, 2009.
- [21] R. Carmona and F. Delarue. *Probabilistic Theory of Mean Field Games with Applications I-II*. Springer, 2018.
- [22] R. Carmona and F. Delarue. *Probabilistic Theory of Mean Field Games with Applications I-II*. Springer, 2018.
- [23] N. Cetorelli, B. Hirtle, D. P. Morgan, S. Peristiani, and J. A. Santos. Trends in financial market concentration and their implications for market stability. *Economic Policy Review*, 13(1), 2007.
- [24] A. Chakraborti, I. M. Toke, M. Patriarca, and F. Abergel. Econophysics review: I. empirical facts. *Quantitative Finance*, 11(7):991–1012, 2011.
- [25] D. R. Chambers and J. S. Zdanowicz. The limitations of diversification return. *The Journal of Portfolio Management*, 40(4):65–76, 2014.
- [26] S. Chatterjee and S. Pal. A phase transition behavior for Brownian motions interacting through their ranks. *Probability Theory and Related Fields*, 147(1-2):123–159, 2010.
- [27] R. Cont. Empirical properties of asset returns: stylized facts and statistical issues. *Quantitative Finance*, 1(2):223, 2001.
- [28] S. Corbet, A. Meegan, C. Larkin, B. Lucey, and L. Yarovaya. Exploring the dynamic relationships between cryptocurrencies and other financial assets. *Economics Letters*, 165:28–34, 2018.
- [29] T. M. Cover. Universal portfolios. *Mathematical finance*, 1(1):1–29, 1991.

[30] Z. Csereklyei, M. d. M. Rubio-Varas, and D. I. Stern. Energy and economic growth: the stylized facts. *The Energy Journal*, 37(2):1–34, 2016.

[31] C. Cuchiero. Polynomial processes in stochastic portfolio theory. *Stochastic processes and their applications*, 129(5):1829–1872, 2019.

[32] C. Cuchiero, G. Gazzani, and S. Svaluto-Ferro. Signature-based models: theory and calibration. *SIAM Journal on Financial Mathematics*, 14(3):910–957, 2023.

[33] C. Cuchiero, M. Larsson, and S. Svaluto-Ferro. Polynomial jump-diffusions on the unit simplex. *Annals of Applied Probability*, 28(4):2451–2500, 2018.

[34] C. Cuchiero and J. Möller. Signature methods in stochastic portfolio theory. *arXiv preprint arXiv:2310.02322*, 2023.

[35] C. Cuchiero, W. Schachermayer, and T.-K. L. Wong. Cover’s universal portfolio, stochastic portfolio theory, and the numéraire portfolio. *Mathematical Finance*, 29(3):773–803, 2019.

[36] J. Cvitanic and I. Karatzas. On portfolio optimization under “drawdown” constraints. 1994.

[37] M. H. Davis. *Mathematical Finance: A Very Short Introduction*. Oxford University Press, 2019.

[38] M. A. Dempster, I. V. Evstigneev, and K. R. Schenk-Hoppé. Volatility-induced financial growth. *Quantitative Finance*, 7(2):151–160, 2007.

[39] C. Ding and H. Qi. An optimization study of diversification return portfolios. *arXiv preprint arXiv:2303.01657*, 2023.

[40] J. J. Egozcue, V. Pawlowsky-Glahn, G. Mateu-Figueras, and C. Barcelo-Vidal. Isometric logratio transformations for compositional data analysis. *Mathematical Geology*, 35(3):279–300, 2003.

[41] M. Émery. *Stochastic Calculus in Manifolds*. Springer, 1989.

[42] I. V. Evstigneev, T. Hens, and K. R. Schenk-Hoppé. Evolutionary finance. *Handbook of financial markets: dynamics and evolution*, pages 507–566, 2009.

[43] E. F. Fama and K. R. French. The cross-section of expected stock returns. *the Journal of Finance*, 47(2):427–465, 1992.

[44] D. Fernholz and I. Karatzas. On optimal arbitrage. *The Annals of Applied Probability*, 20(4):1179–1204, 2010.

[45] D. Fernholz and I. Karatzas. Probabilistic aspects of arbitrage. In *Contemporary Quantitative Finance: Essays in Honour of Eckhard Platen*, pages 1–17. Springer, 2010.

[46] D. Fernholz and I. Karatzas. Optimal arbitrage under model uncertainty. *The Annals of Applied Probability*, 21(6):2191–2225, 2011.

[47] E. R. Fernholz. *Stochastic Portfolio Theory*. Springer, 2002.

[48] E. R. Fernholz, I. Karatzas, and J. Ruf. Volatility and arbitrage. *The Annals of Applied Probability*, 28(1):378–417, 2018.

[49] R. Fernholz. On the diversity of equity markets. *Journal of Mathematical Economics*, 31(3):393–417, 1999.

[50] R. Fernholz. Portfolio generating functions. In *Quantitative Analysis in Financial Markets: Collected Papers of the New York University Mathematical Finance Seminar*, pages 344–367. World Scientific, 1999.

[51] R. Fernholz. E. Robert Fernholz, PhD: Stochastic Portfolio Theory. *Journal of Investment Consulting*, 20(1):12–20, 2020.

[52] R. Fernholz and R. Garvy. Diversity changes affect relative performance. *Pensions & Investments*, 112, 1999.

[53] R. Fernholz, R. Garvy, and J. Hannon. Diversity-weighted indexing. *Journal of Portfolio Management*, 24(2):74, 1998.

[54] R. Fernholz, T. Ichiba, and I. Karatzas. A second-order stock market model. *Annals of Finance*, 9:439–454, 2013.

[55] R. Fernholz and I. Karatzas. Relative arbitrage in volatility-stabilized markets. *Annals of Finance*, 1(2):149–177, 2005.

[56] R. Fernholz and I. Karatzas. Stochastic portfolio theory: an overview. *Handbook of numerical analysis*, 15(89–167):1180–91267, 2009.

[57] R. Fernholz and C. Maguire Jr. The statistics of statistical arbitrage. *Financial Analysts Journal*, 63(5):46–52, 2007.

[58] R. Fernholz and B. Shay. Stochastic portfolio theory and stock market equilibrium. *The Journal of Finance*, 37(2):615–624, 1982.

[59] R. T. Fernholz and R. Fernholz. Zipf’s law for atlas models. *Journal of Applied Probability*, 57(4):1276–1297, 2020.

[60] R. T. Fernholz and R. Fernholz. Portfolios generated by contingent claim functions, with applications to option pricing. *arXiv preprint arXiv:2308.13717*, 2023.

[61] W. Ferson. *Empirical Asset Pricing: Models and Methods*. MIT Press, 2019.

[62] X. Gabaix. Zipf’s law for cities: an explanation. *The Quarterly Journal of Economics*, 114(3):739–767, 1999.

[63] J. Gatheral, T. Jaisson, and M. Rosenbaum. Volatility is rough. *Quantitative finance*, 18(6):933–949, 2018.

[64] M. D. Gould, M. A. Porter, S. Williams, M. McDonald, D. J. Fenn, and S. D. Howison. Limit order books. *Quantitative Finance*, 13(11):1709–1742, 2013.

[65] S. Gu, B. Kelly, and D. Xiu. Empirical asset pricing via machine learning. *The Review of Financial Studies*, 33(5):2223–2273, 2020.

[66] M. Huang, P. E. Caines, and R. P. Malhamé. Large-population cost-coupled LQG problems with nonuniform agents: individual-mass behavior and decentralized ϵ -Nash equilibria. *IEEE transactions on automatic control*, 52(9):1560–1571, 2007.

[67] M. Huang, R. P. Malhamé, P. E. Caines, et al. Large population stochastic dynamic games: closed-loop McKean–Vlasov systems and the Nash certainty equivalence principle. *Communications in Information & Systems*, 6(3):221–252, 2006.

[68] T. Ichiba, I. Karatzas, and M. Shkolnikov. Strong solutions of stochastic equations with rank-based coefficients. *Probability Theory and Related Fields*, 156(1-2):229–248, 2013.

[69] T. Ichiba, V. Papathanakos, A. Banner, I. Karatzas, and R. Fernholz. Hybrid Atlas models. *The Annals of Applied Probability*, 21(2):609–644, 2011.

[70] T. Ichiba and T. Yang. Relative arbitrage opportunities in n investors and mean-field regimes. *arXiv preprint arXiv:2006.15158*, 2020.

[71] D. Itkin, B. Koch, M. Larsson, and J. Teichmann. Ergodic robust maximization of asymptotic growth under stochastic volatility. *arXiv preprint arXiv:2211.15628*, 2022.

[72] D. Itkin and M. Larsson. Robust asymptotic growth in stochastic portfolio theory under long-only constraints. *Mathematical Finance*, 32(1):114–171, 2022.

[73] D. Itkin and M. Larsson. Calibrated rank volatility stabilized models for large equity markets. *arXiv preprint arXiv:2403.04674*, 2024.

[74] D. Itkin and M. Larsson. Open markets and hybrid Jacobi processes. *The Annals of Applied Probability*, 34(3):2940–2985, 2024.

[75] Z. Jian and X. Li. Skewness-based market integration: A systemic risk measure across international equity markets. *International Review of Financial Analysis*, 74:101664, 2021.

[76] J. Kakeu and R. Foguen Tchuendom. Size distribution of firms and strategic investments in large markets: a stochastic mean field game approach. *SSRN*, 2022.

[77] I. Karatzas and C. Kardaras. *Portfolio Theory and Arbitrage: A Course in Mathematical Finance*, volume 214. American Mathematical Society, 2021.

[78] I. Karatzas and D. Kim. Open markets. *Mathematical Finance*, 31(4):1111–1161, 2021.

[79] I. Karatzas and J. Ruf. Trading strategies generated by Lyapunov functions. *Finance and Stochastics*, 21(3):753–787, 2017.

[80] I. Karatzas and A. Sarantsev. Diverse market models of competing brownian particles with splits and mergers. *Annals of Applied Probability*, 26(3):1329–1361, 2016.

[81] C. Kardaras and S. Robertson. Robust maximization of asymptotic growth. *The Annals of Applied Probability*, 22(4):1576–1610, 2012.

[82] C. Kardaras and S. Robertson. Ergodic robust maximization of asymptotic growth. *The Annals of Applied Probability*, 31(4):1787–1819, 2021.

[83] D. Kim. Market-to-book ratio in stochastic portfolio theory. *Finance and Stochastics*, 27(2):401–434, 2023.

[84] P. Kolli and A. Sarantsev. Large rank-based models with common noise. *Statistics & Probability Letters*, 151:29–35, 2019.

[85] J.-M. Lasry and P.-L. Lions. Mean field games. *Japanese Journal of Mathematics*, 2(1):229–260, 2007.

[86] T. Leinster. *Entropy and Diversity: The Axiomatic Approach*. Cambridge University Press, 2021.

[87] X. Li, T.-K. L. Wong, R. T. Chen, and D. Duvenaud. Scalable gradients for stochastic differential equations. In *International Conference on Artificial Intelligence and Statistics*, pages 3870–3882. PMLR, 2020.

[88] O. Linton. *Financial Econometrics*. Cambridge University Press, 2019.

[89] P. Mackintosh. How much does trading cost the buy side? <https://www.nasdaq.com/articles/how-much-does-trading-cost-the-buy-side>, 2022.

[90] R. Malladi and F. J. Fabozzi. Equal-weighted strategy: Why it outperforms value-weighted strategies? theory and evidence. *Journal of Asset Management*, 18:188–208, 2017.

[91] D. Mantilla-Garcia, J. Malagon, and J. R. Aldana-Galindo. Can the portfolio excess growth rate explain the predictive power of idiosyncratic volatility? *Finance Research Letters*, 47:102577, 2022.

[92] R. C. Merton. Lifetime portfolio selection under uncertainty: The continuous-time case. *The Review of Economics and Statistics*, pages 247–257, 1969.

[93] S. A. A. Monter, M. Shkolnikov, and J. Zhang. Dynamics of observables in rank-based models and performance of functionally generated portfolios. *The Annals of Applied Probability*, 29(5):2849–2883, 2019.

[94] M. E. Newman. Power laws, Pareto distributions and Zipf’s law. *Contemporary Physics*, 46(5):323–351, 2005.

[95] S. Pal. Analysis of market weights under volatility-stabilized market models. *The Annals of Applied Probability*, 21(3):1180–1213, 2011.

[96] S. Pal and T.-K. L. Wong. Energy, entropy, and arbitrage. *arXiv preprint arXiv:1308.5376*, 2013.

[97] S. Pal and T.-K. L. Wong. The geometry of relative arbitrage. *Mathematics and Financial Economics*, 10(3):263–293, 2016.

[98] S. Pal and T.-K. L. Wong. Exponentially concave functions and a new information geometry. *The Annals of Probability*, 46(2):1070–1113, 2018.

[99] M. S. Paoletta and L. Taschini. An econometric analysis of emission allowance prices. *Journal of Banking & Finance*, 32(10):2022–2032, 2008.

[100] E. Platen and R. Rendek. Approximating the numéraire portfolio by naive diversification. *Journal of Asset Management*, 13:34–50, 2012.

[101] Y. Plyakha, R. Uppal, and G. Vilkov. Why does an equal-weighted portfolio outperform value-and price-weighted portfolios? *Available at SSRN 2724535*, 2012.

[102] E. E. Qian. *Portfolio Rebalancing*. CRC Press, 2018.

[103] D. Revuz and M. Yor. *Continuous Martingales and Brownian Motion*. Springer, third edition, 1999.

[104] J. Ruf. Empirical Finance with Equity Data (Ph.D. Course). https://github.com/johruf/CRSP_on_WRDS_introduction, 2024. London School of Economics and Political Science.

[105] J. Ruf and K. Xie. The impact of proportional transaction costs on systematically generated portfolios. *SIAM Journal on Financial Mathematics*, 11(3):881–896, 2020.

[106] A. I. Saichev, Y. Malevergne, and D. Sornette. *Theory of Zipf's Law and Beyond*. Springer Science & Business Media, 2009.

[107] Y.-L. K. Samo and A. Vervuurt. Stochastic portfolio theory: A machine learning perspective. *arXiv preprint arXiv:1605.02654*, 2016.

[108] A. Sarantsev and L.-C. Tsai. Stationary gap distributions for infinite systems of competing Brownian particles. *Electronic Journal of Probability*, 22(56):1–20, 2017.

[109] M. Shkolnikov and L. C. Yung. From rank-based models with common noise to pathwise entropy solutions of SPDEs. *arXiv preprint arXiv:2406.07286*, 2024.

[110] L. Shu, F. Shi, and G. Tian. High-dimensional index tracking based on the adaptive elastic net. *Quantitative Finance*, 20(9):1513–1530, 2020.

[111] B. H. Taljaard and E. Mare. Why has the equal weight portfolio underperformed and what can we do about it? *Quantitative Finance*, 21(11):1855–1868, 2021.

[112] S. Thurner, R. Hanel, and P. Klimek. *Introduction to the Theory of Complex Systems*. Oxford University Press, 2018.

[113] R. S. Tsay. *Analysis of Financial Time Series*. John Wiley & Sons, third edition, 2010.

[114] A. Vervuurt and I. Karatzas. Diversity-weighted portfolios with negative parameter. *Annals of Finance*, 11:411–432, 2015.

[115] L. Wang. Fund pros burned in AI surge are giving up on active management. *Bloomberg*, 2024. Available at: <https://www.bloomberg.com/news/articles/2024-01-22/fund-pros-burned-in-ai-surge-are-giving-up-on-active-management>.

[116] S. Willenbrock. Diversification return, portfolio rebalancing, and the commodity return puzzle. *Financial Analysts Journal*, 67(4):42–49, 2011.

[117] T.-K. L. Wong. Optimization of relative arbitrage. *Annals of Finance*, 11(3-4):345–382, 2015.

[118] T.-K. L. Wong. Universal portfolios in stochastic portfolio theory. *arXiv preprint arXiv:1510.02808*, pages 1–25, 2015.

[119] T.-K. L. Wong. Information geometry in portfolio theory. In *Geometric Structures of Information*, pages 105–136. Springer, 2019.

[120] K. Xie. Leakage of rank-dependent functionally generated trading strategies. *Annals of Finance*, 16(4):573–591, 2020.

[121] C. Zhang, P. Kokoszka, and A. Petersen. Wasserstein autoregressive models for density time series. *Journal of Time Series Analysis*, 43(1):30–52, 2022.

[122] W. Zhang, P. Wang, X. Li, and D. Shen. Some stylized facts of the cryptocurrency market. *Applied Economics*, 50(55):5950–5965, 2018.

[123] Z. Zhang, S. Zohren, and S. Roberts. Deep learning for portfolio optimization. *arXiv preprint arXiv:2005.13665*, 2020.

COLUMBIA UNIVERSITY
Email address: sc5314@columbia.edu

UNIVERSITY OF TORONTO
Email address: johnsqe.song@alumni.utoronto.ca

UNIVERSITY OF TORONTO
Email address: tkl.wong@utoronto.ca